Master's Thesis

A Study on the Effects of Inactive Materials in Slurry and Electrode Structure on Rapid Charge of Lithium-ion Battery

Younghye Kang

Department of Energy Engineering

(Battery Science and Technology)

Graduate School of UNIST

2018

A Study on the Effects of Inactive Materials in Slurry and Electrode Structure on Rapid Charge of Lithium-ion Battery

Younghye Kang

Department of Energy Engineering
(Battery Science and Technology)

Graduate School of UNIST

A Study on the Effects of Inactive Materials in Slurry and Electrode Structure on Rapid Charge of Lithium-ion Battery

A thesis/dissertation
submitted to the Graduate School of UNIST
in partial fulfillment of the
requirements for the degree of
Master of Science

Younghye Kang

12.18.2017

Approved by

Advisor
Kyeong-Min Jeong

A Study on the Effects of Inactive Materials in Slurry and Electrode Structure on Rapid Charge of Lithium-ion Battery

Younghye Kang

This certifies that the thesis/dissertation of Younghye Kang is approved.

12.18.2017

Advisor: Kyeong-Min Jeong

Jaephil Cho

Nam-Soon Choi

Contents

Abstract

Lithium ion battery electrode is porous electrode consists of various components such as active material, binder and conducting agent. Among them, binder and conducting agent are inactive part so that they cannot assist active material directly to implement capacity but constitute electrode and help active material working.

Many researches tried to find out optimized ratio of inactive components for each active materials. Those researches tried too high ratio of binder or conducting agent for noticeable difference in results which cannot applied to market production. In this study, it will be described that cell performance comes from not only active material but also effect of inactive materials. It will show that slight difference of inactive material ratio in slurry can result extensive difference in electrode performance.

CMC thickner and SBR binder are essential components in commercialized lithium ion battery anode. Since binding structure of CMC is wrapping active material particles, CMC has higher possibility to interfere ionic, electronic conductivity compare to SBR, under the condition of consistent active material ratio. In cathode, PVDF binder has similar binding structure with CMC in anode so that it also can resist ionic, electronic conduction. To confirm those assumptions, graphite anode slurry were mixed with total ratio of 2.6% binder. Experiment were done with three different ratio; 0.6% CMC with 2% SBR, 1.2% CMC with 1.4% SBR, 2% CMC with 0.6% SBR. The active material ratio were all maintained equally for each of the three samples. NCM622 cathode were mixed with different ratio and conducting agents. KF9300 (Kureha) were used as binder and Super P and Ketjen Black were used as conducting agent. The slurry mixed with two different ratio of binder and conducting agent; 2% binder with 2% conducting agent and 2.5% binder with 1.5% conducting agent. Active material ratio was fixed as 96% for all samples.

From the observation of freeze dried slurry, it was possible to confirm that CMC binder wrapping graphite particles in anode and PVDF binder wrapping NCM particles in cathode. High CMC ratio electrode has higher physical binding strength but lower initial charge, discharge capacity compare to high SBR ratio electrode. For rapid charge cycles, cell with high CMC ratio electrode showed higher cycle retention compared to cell with high SBR ratio electrode. Cathode with high PVDF ratio shows higher mechanical binding strength and higher resistance. Cathode with Ketjen Black conducting agent shows lower binding strength and lower resistance compare to cathode with Super P conducting agent. Those results shows that binding structure of binder and conducting agent affect cell performance both physically and electrochemically. To achieve rapid charge in LIB, it is important to achieve appropriate binding structures by using inactive material properties.

List of Figures

List of Tables

Ⅰ. Introduction

1.1. Lithium-ion batteries

Lithium ion secondary battery has been used for over 20 years because of its high gravimetric energy density and power density as shown in Figure 1. Lithium ion battery uses lithium, the lightest metal on the earth and uses organic electrolyte so that the working voltage window is large enough compare to other battery systems. With the development of portable electronic devices, usage of lithium ion battery has been extended from a digital camera to electric vehicles.

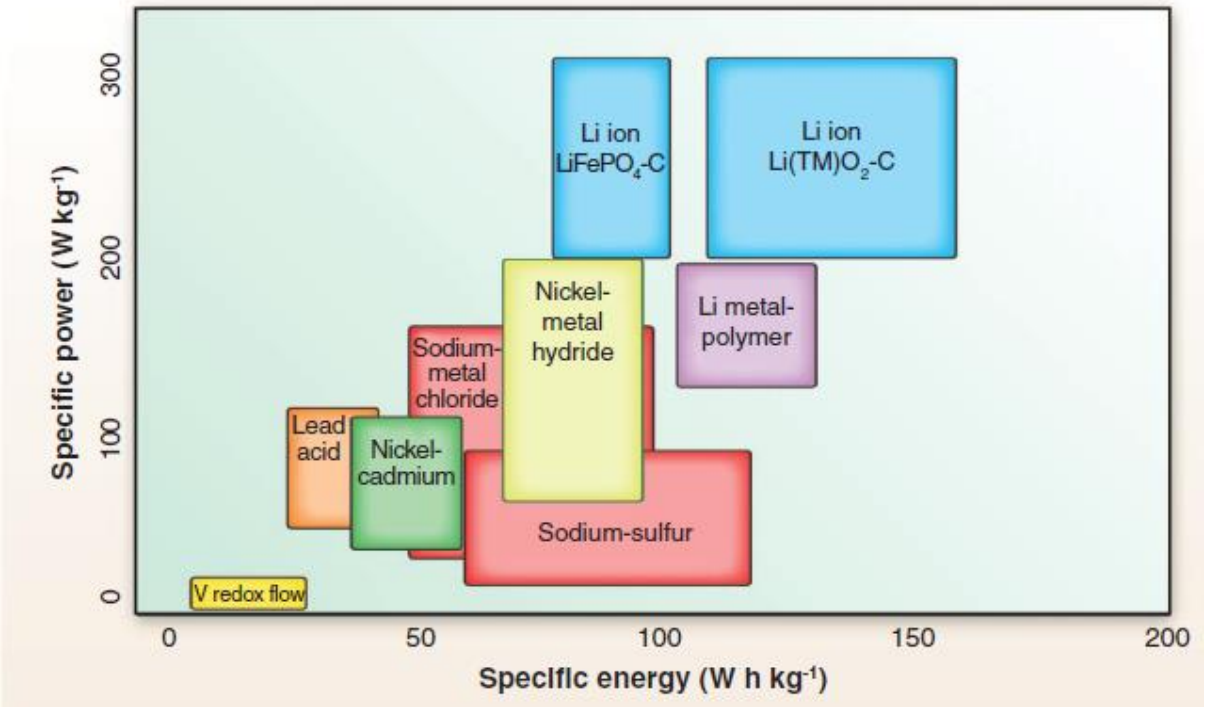

Figure 1. Gravimetric power densities and energy densities for different rechargeable batteries. [5]

According to Bloomberg report, the price of an electric vehicle will be similar to an internal-combustion engine vehicle early in 2022 and the market share of the global electric vehicle would be increases from 1% to 35% in 2040. Lithium ion battery for the electric vehicle should satisfy long mileage and sufficient power to compete against to the internal-combustion engine vehicle, therefore it needs high energy density and high power characteristics. Also, the rapid charge of the lithium ion battery is important to realize charging time of the electric vehicle similar to fueling of the internal combustion engine vehicle.

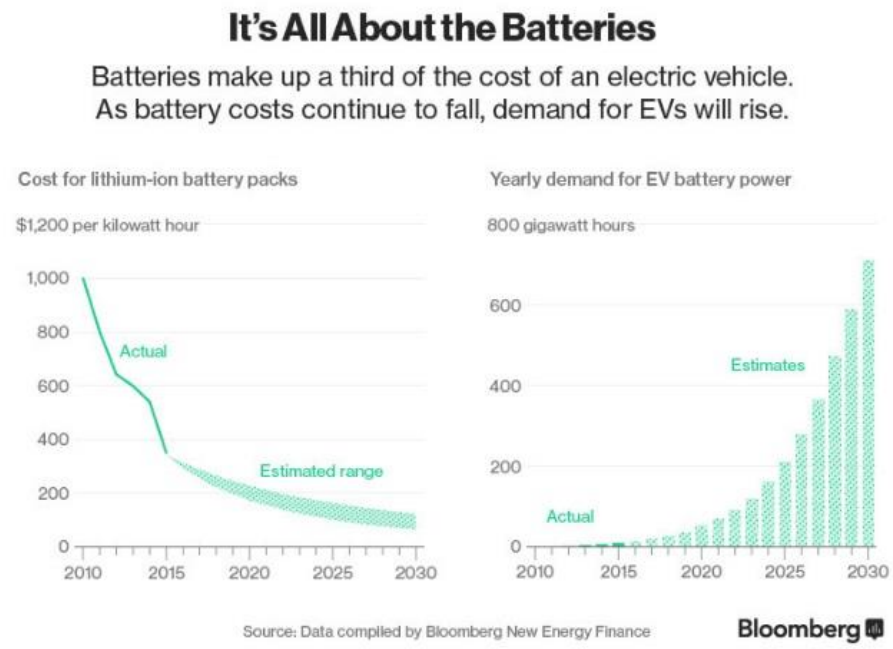

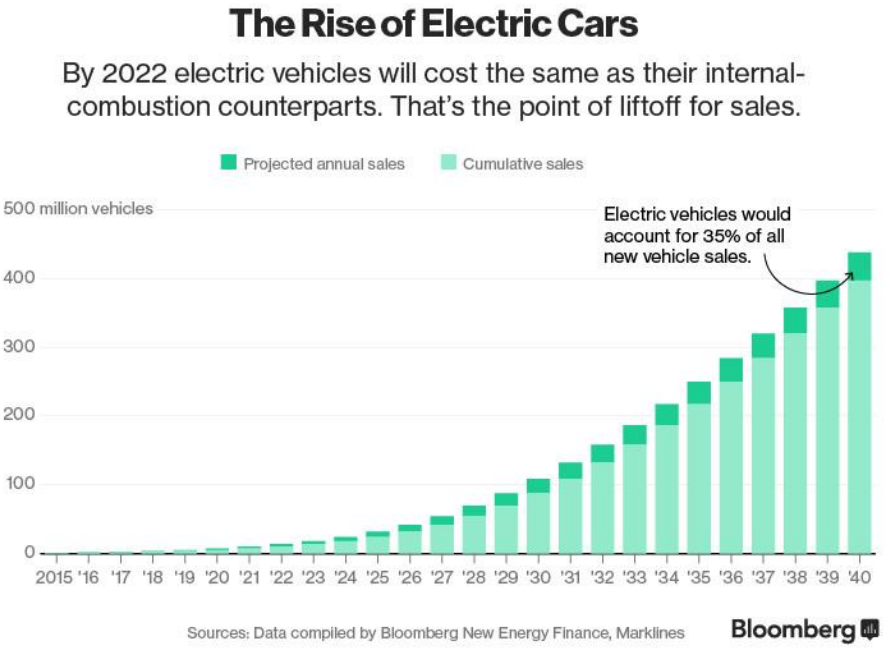

Figure 2. Bloomberg report.

https://www.bloomberg.com/features/2016-ev-oil-crisis/

1.2. Researches about lithium-ion battery

Lithium ion battery stores and uses electric energy during oxidation and reduction of transition metal in cathode. In charging process, cell voltage increases while lithium ion moves from cathode to anode. In discharging process, lithium ion moves from anode to cathode and cell voltage decreases. Both cathode and anode of the commercialized lithium ion battery intercalates lithium ion during charge and discharge. Figure 3 is a schematic illustration of the Li-ion battery using $LiCoO_2$ cathode and graphite anode.

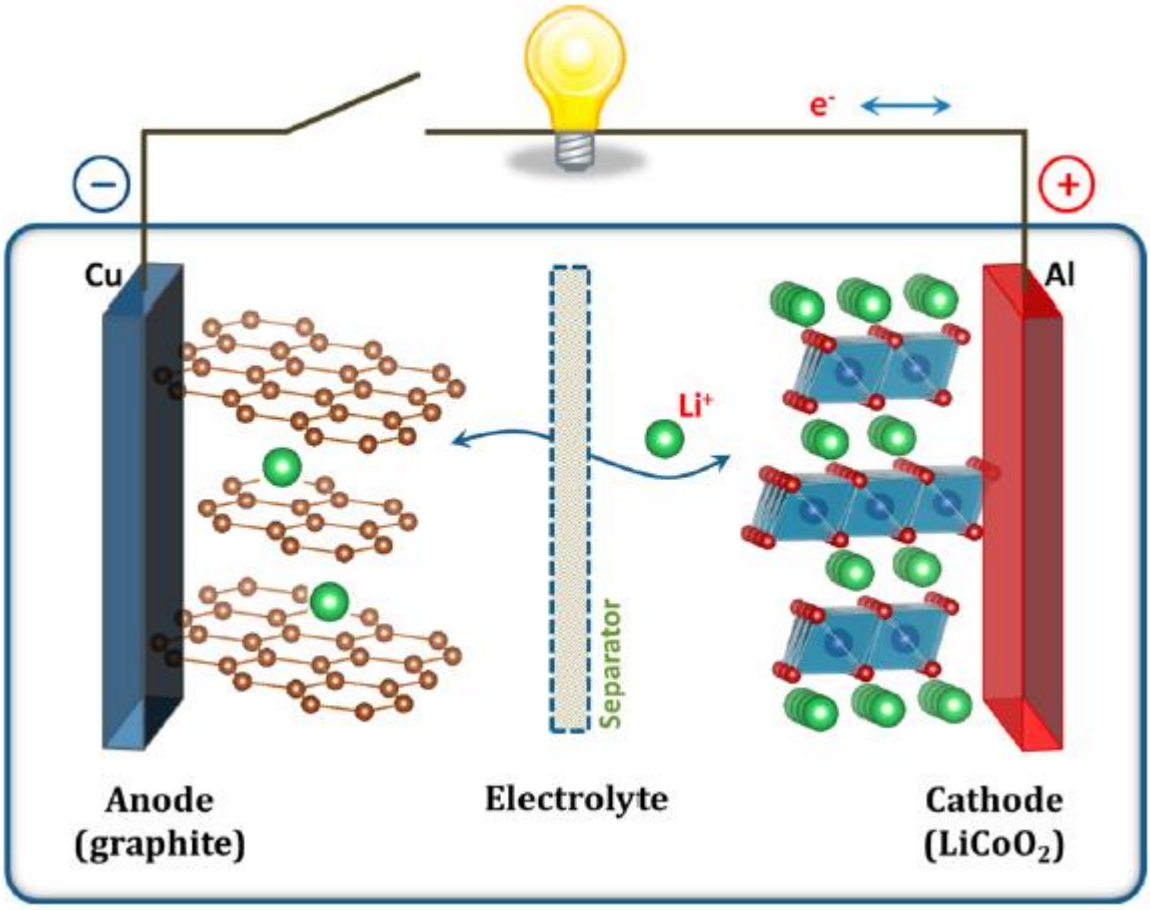

Figure 3. Schematic illustration of the Li-ion battery. [4]

1.2.1. Active material

Developing and improving active material has been actively researched by many research groups. The first lithium ion battery was developed in 1980 by Goodenough, using $LiCoO_2$ as cathode.[16] In 1982, Yazami used graphite as anode.[17] In 1985, a prototype lithium ion battery using $LiCoO_2$ and graphite was developed by Yoshino.[18] The first commercialization of the lithium ion battery was in 1990 by Sony Corporation.[19]

$LiCoO_2$ has layered structure and lithium can be removed electrochemically during charging.[20-22] It has the theoretical gravimetric capacity of 274mAh/g but commonly usable capacity is about 150 to 170mAh/g to avoid structure collapse. Graphite has several graphene layers consist of carbon. It has the gravimetric capacity of 372mAh/g. In these days, $Li[NiCoMn]O_2$ or $Li[NiCoAl]O_2$ cathode and Silicon-graphite composite anode have been developed as the lithium ion battery active material for electric vehicle. $Li[NiCoMn]O_2$ and $Li[NiCoAl]O_2$ cathode have higher specific capacity compare to $LiCoO_2$ because of nickel which has two steps of oxidation in charge state.[7, 23-24] Figure 4 shows the specific capacity of various cathode materials. Silicon-graphite composite anode has higher specific capacity compared to graphite anode because Silicon has a higher theoretical capacity of 4200mAh/g.[12, 25] However, since Silicon undergoes severe volume expansion during charging, making composites of Silicon and graphite has been suggested as the alternative method to increase capacity and prevent severe volume expansion.[8]

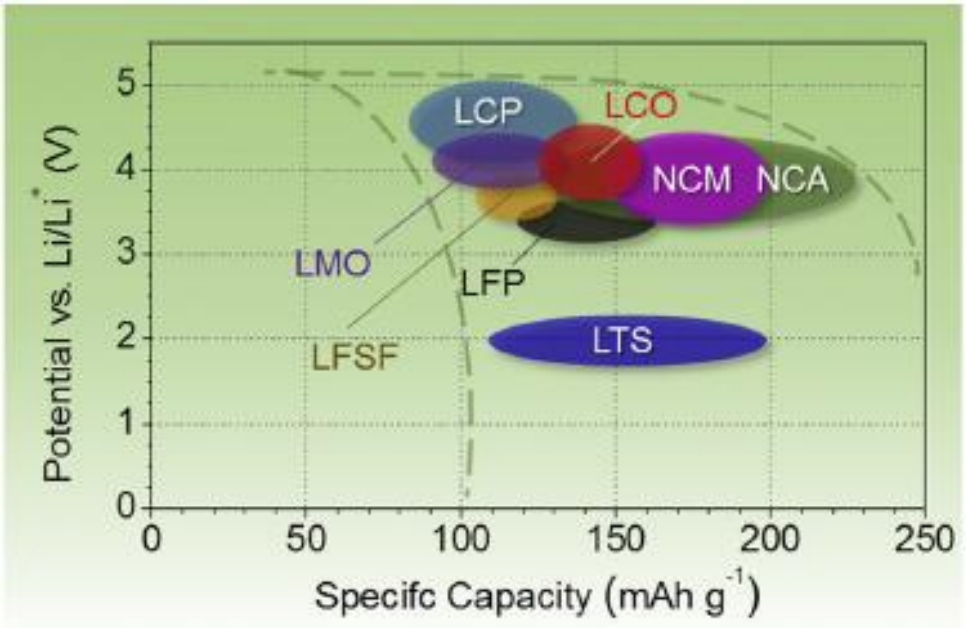

Figure 4. Approximate range of average potentials and specific capacity of common intercalation-type cathodes. [7]

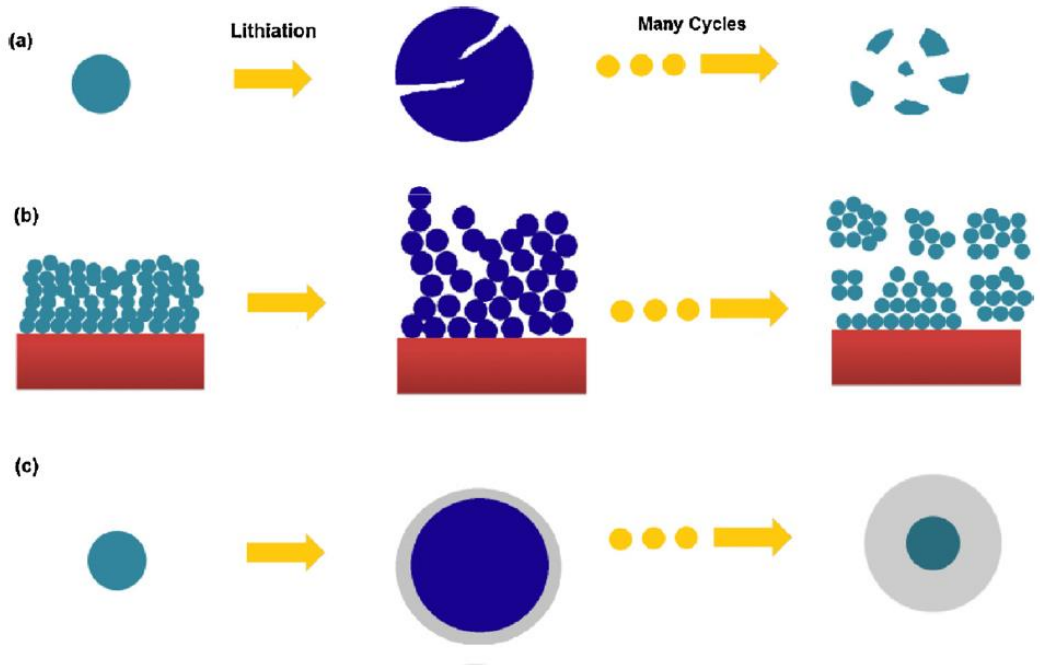

Figure 5. Failure mechanism of Si electrode: (a) pulverization of material. (b) Morphology and volume change of the entire Si electrode. (c) Continuous SEI growth.[8]

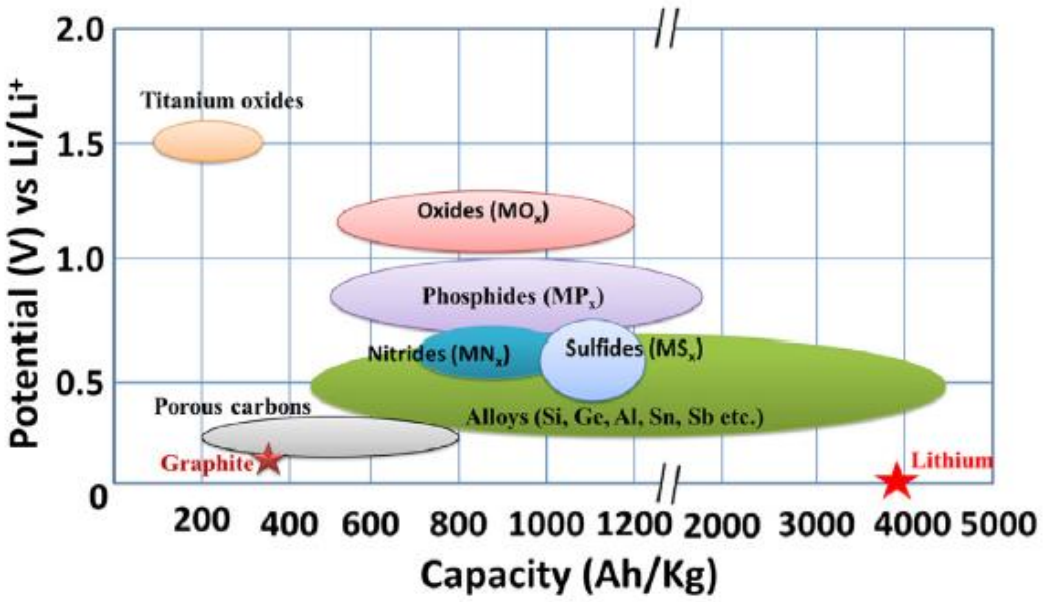

Figure 6. Schematic illustration of potential and capacity of anode materials for the next generation of lithium batteries. [12]

1.2.2. Electrochemistry

The energy density of the lithium ion battery is determined by three factors which are cell voltage (V_{cell}), gravimetric capacity (Ah/kg) and density (mg/cm^3). The relationship between energy density and those three factors is shown in below.

Working specific energy density = (Cell voltage) x (Specific capacity) / (Mass loading) / (Thickness)
= (Cell voltage - Overvoltage) x (Specific capacity) / (Mass loading) / (Thickness)

$$Wh/_{L} = V_{cell} \cdot Ah \Big/ kg \cdot \frac{L}{kg}$$
$$= V_{cell} \cdot Ah/_{kg} \times d$$
$$= (V_{cell} - \eta_s - \eta_c - \phi_{IR}) \cdot Ah/_{kg} \times d$$
$$= (V_{cell} - \eta_s - \eta_c - \phi_{IR}) \cdot Ah/_{kg} \times mg/cm^2 \times 1/cm$$

To increase the energy density of the cell, increasing cell voltage is needed. Decreasing overpotential of the cell can increase cell voltage and therefore, increase energy density. The overpotential of the cell is defined as the additional potential beyond the thermodynamic requirement needed to drive a reaction at a certain rate.[26] Overpotential can be classified in three categories which are resistance overpotential, charge transfer overpotential or activation overpotential, and concentration overpotential.[6]

Resistance overpotential which arises from ohmic drop, depends on the conductivity of electrolyte solution.[1] Charge transfer overpotential or activation overpotential occurs during electrode reaction. When charge transfer reaction proceeds, it needs to overcome some barrier. This barrier is activation barrier or activation overpotential. The magnitude of it depends on several factors such as material property, active area, reaction type and so on. Concentration variation in electrolyte solution leads to the potential difference between two electrodes. Concentration gradient in the solution cause concentration overpotential which leads to the voltage drop. If the concentration of solution is low, it needs higher concentration overpotential compare to high concentration solution because it has higher mass transfer resistance.

By decreasing those overpotential, it is possible to increase the energy density of a cell. Also rate capability of the cell can be improved. The high ionic conductivity of electrolyte solution and well-developed electrode structure can lower resistance overpotential and concentration overpotential. The electrode structure of porous electrode can affect charge transfer overpotential, so well-developed electrode structure would lower either resistance overpotential and charge transfer overpotential.

1.2.3. Factors influence lithium ion battery performance

Lithium ion battery performance can be influenced by many factors. Not only active material and electrolyte but also production process determine battery performance including capacity, cycle retention, rate capability and so on. The production process includes mixing, coating, pressing and drying. Assembling and formation conditions also influence cell performance. Figure 7 shows schematic illustration of process-structure-property relations in lithium-ion battery electrodes.

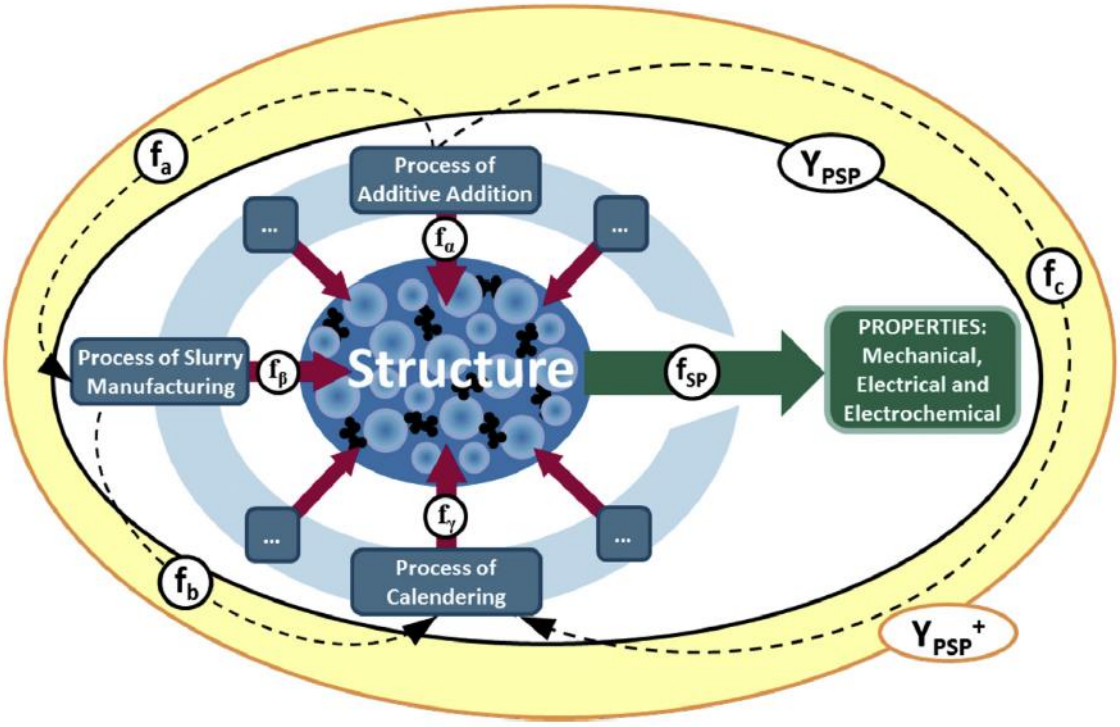

Figure 7 Schematic illustration of manufacturing process-electrode structure-cell property relations in lithium-ion battery electrodes.[27]

During the mixing process, the dispersion of slurry is determined. Uniform slurry condition is important for cell performance. When the carbon conducting agent is included in the slurry, uniform dispersion of conducting agent is being more critical. Heterogeneous composite condition can result uneven current density in the electrode composite which cause high overpotential during charge and discharge. Figure 8 shows the schematics of possible impact of carbon black conducting agent on kinetics of Li+/electron electrochemical insertion into active particles. Since the electronic and ionic conductivity of the electrode is influenced by slurry dispersion, many researches have been proceeded changing mixing time or sequence to improve slurry dispersion.

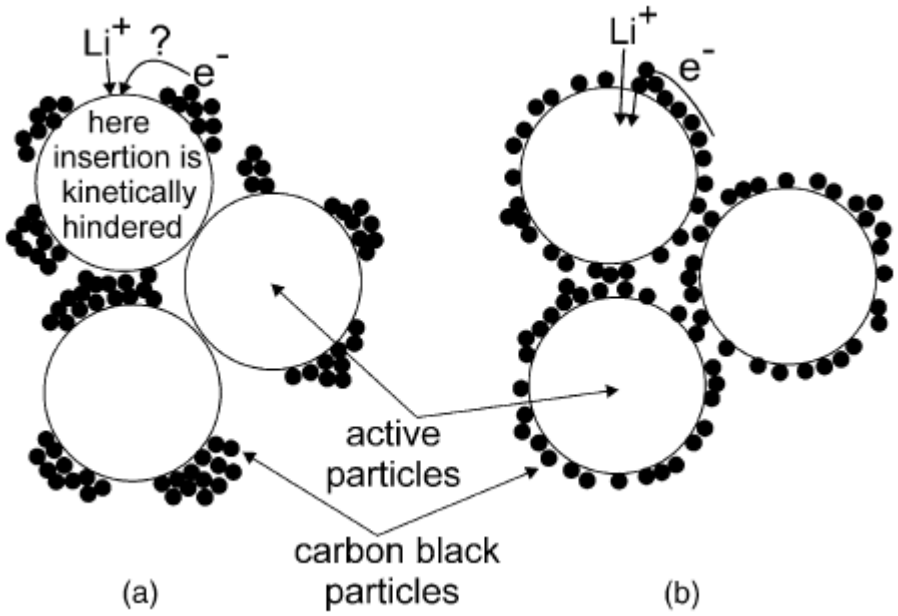

Figure 8. A sketch indicating the possible impact of carbon conducting agent on kinetics of Li+ and electron electrochemical insertion into active particles. [13]

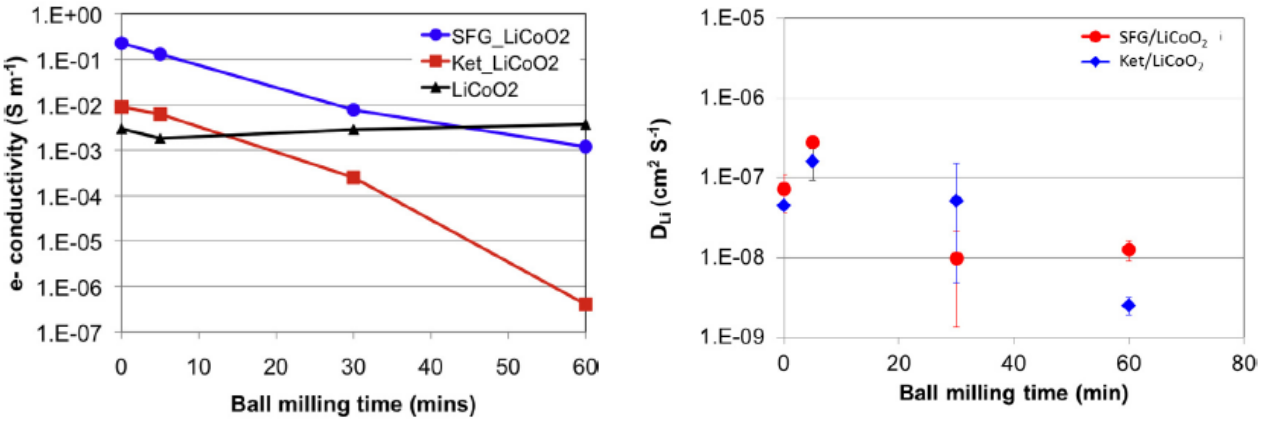

Figure 9. Electronic conductivity of LCO and carbon composite according to ball-milling time (left) and of Lithium diffusivity of LCO and carbon composite according to ball-milling time(right).[14]

During the drying process, slurry solvent evaporates. At this step, appropriate temperature and hot air is needed. If the temperature is too high, evaporate speed is too fast that light conducting agent in slurry can rise to the surface as shown in Figure 10. Also, too high temperature drying results low adhesion strength and high resistance of the electrode as shown in Figure 11.

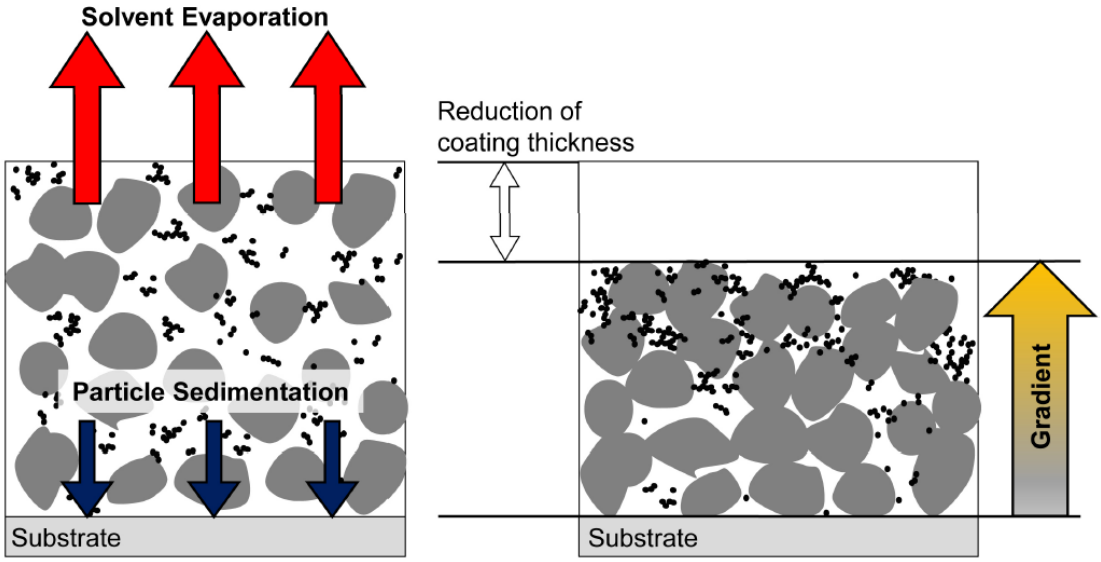

Figure 10. Schematic drawing of the solvent evaporation and particle sedimentation in electrodes for lithium-ion batteries during drying. [10]

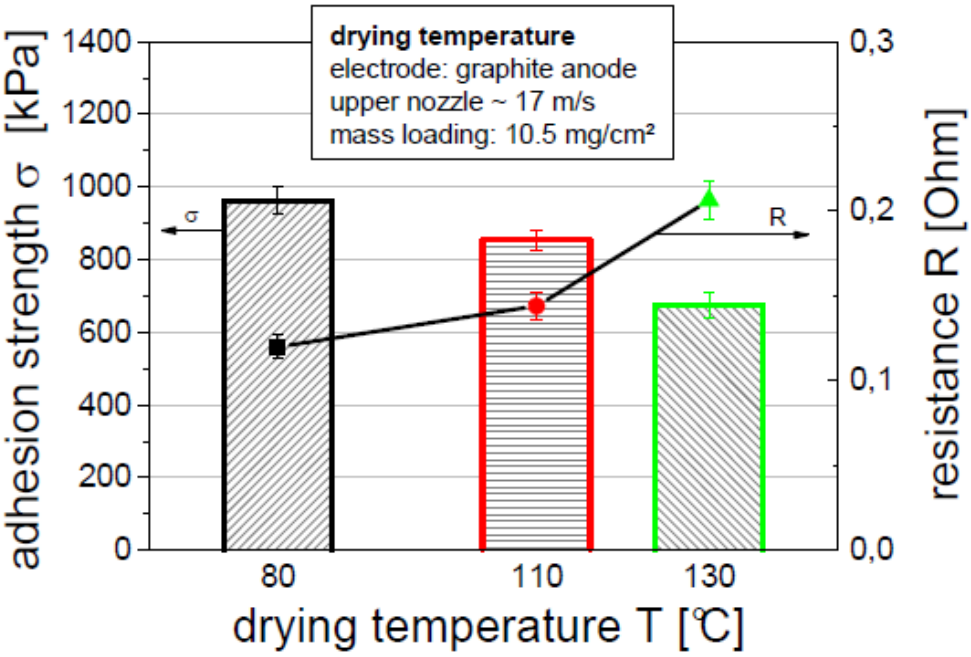

Figure 11. Decreasing adhesion strength and increasing resistance with increasing drying temperature. [6]

Electrode porosity is determined by electrode density. Pressing of electrode is critical because porosity is related to electrode tortuosity which is connected to the lithium ion movement in the electrode composite. High porosity results high impregnation of electrolyte and high rate capability. However, since high porosity results low electrode density and high DC-IR as shown in figure 12, the total energy density of electrode and cell would be lower than low porosity electrode and cell. Figure 13 shows energy density according to porosity and electrode thickness. Figure 14 is cycle performance of cathode at different porosities.

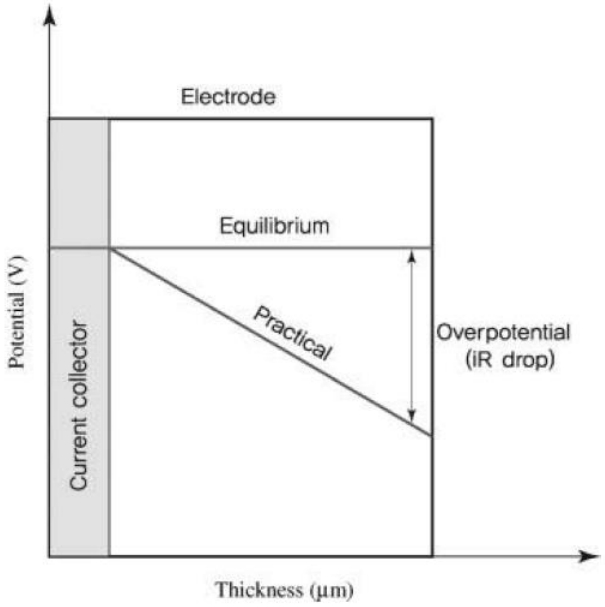

Figure 12. iR drop within a thick electrode.[1]

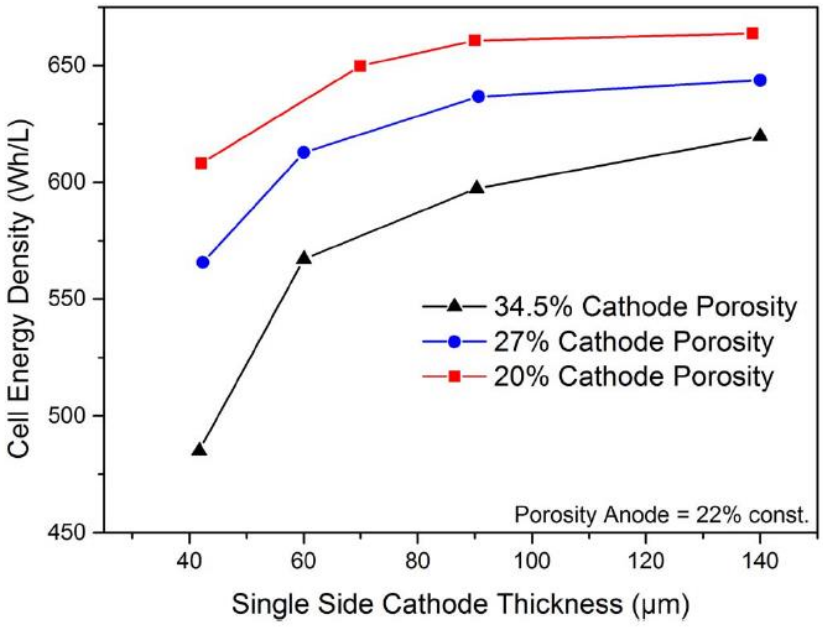

Figure 13. Energy density according to cathode porosity and electrode thickness.[15]

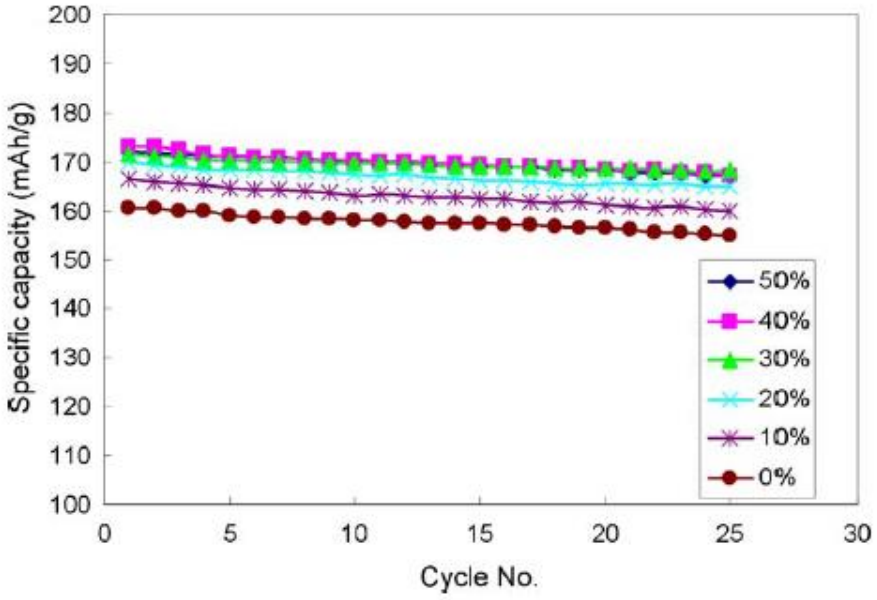

Figure 14. Cycle life of the Li[Ni1/3Mn1/3Co1/3]O2 cathode at different porosities at 0.1C charge and 0.1C.[2]

1.3. Researches about commercialized lithium-ion battery binder

Developing a good electrode structure is as important as improving active material to enable rapid charge capability because uniform charge distribution of electrode can lower overpotential during high rate charge. Many researchers tried various effort to improve lithium ion battery electrode structure to make uniform and non-resistive electrode. Especially binder and conducting agent have been widely researched. Lithium ion battery binder bonds active material and conducting agent together and attach composite on metal substrate. Conducting agent makes conducting network in electrode composite to enable electron conduction from substrate to active material particles.

In cathode, N.-S. Choi and researchers confirmed the effect of polymeric binder in lithium rechargeable battery in 2002.[9] The electrical conductivity of cathode with various PVDF contents were measured and impedance spectra of unit cell (Li/polymer electrolyte/$LiCoO_2$) as the function of PVDF content were also measured. The electrical resistance of cathode and impedance of unit cell were decreased with the increase of PVDF content until certain PVDF content level because binder absorbed liquid electrolyte so that migration of free ion were faster in case of high PVDF content.

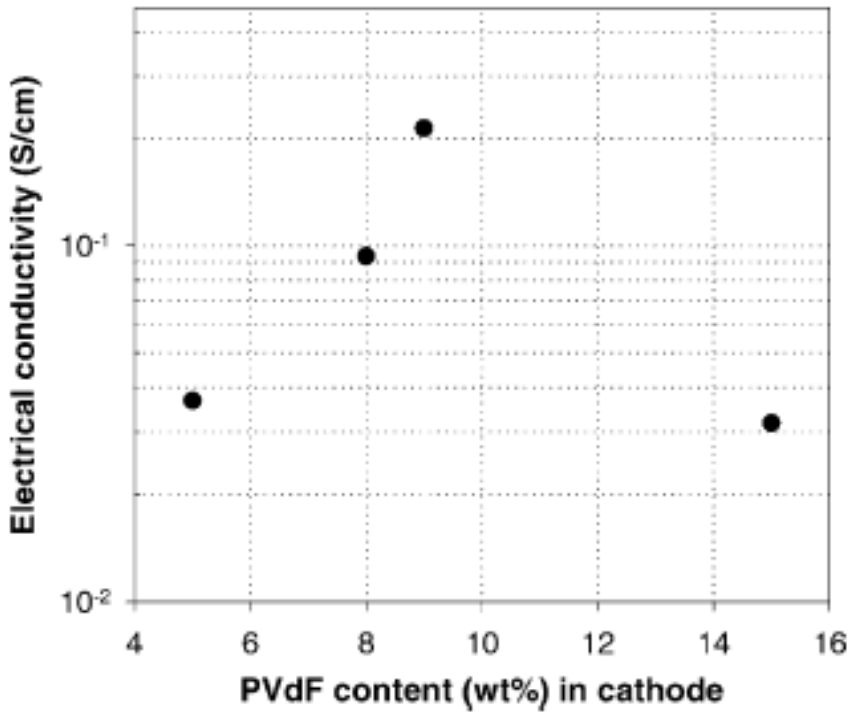

Figure 15. Electrical conductivities of cathode according to PVdF contents.[9]

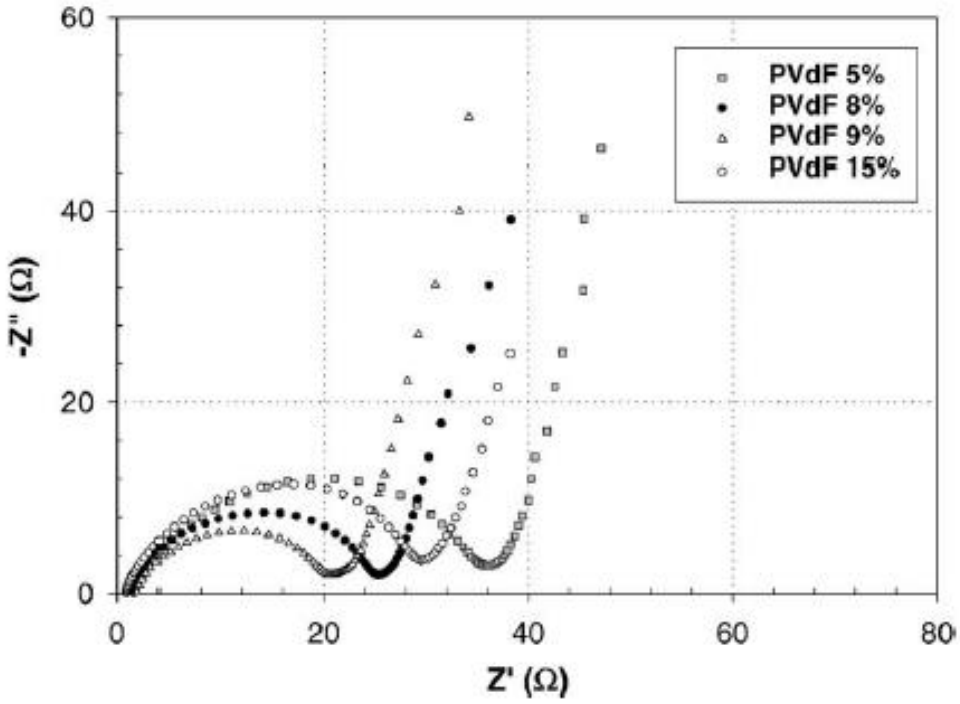

Figure 16. Impedance spectra of cathode unit cell as function of PVdF content .[9]

G. Liu and researchers researched the optimized ratio of acetylene black conducting agent and PVDF binder composition for $LiNi_{0.8}Co_{0.15}Al_{0.05}O_2$ cathode.[28] They also experimented porosity effect. Honghe Zheng et al. also tried to optimize PVDF binder and acetylene black (AB) ratio, focusing on electronic conductivity and breaking stress of composite film.[11] They experimented different ratios from 5:0 to 5:5 of PVDF/AB ratio and found out that when AB ratio increases, electronic conductivity increases and breaking stress decreases. Gravimetric capacity increases when PVDF ratio is fixed and AB ratio increases. Capacity retention of full cell was best when 8% of PVDF and 4.8% of AB used.

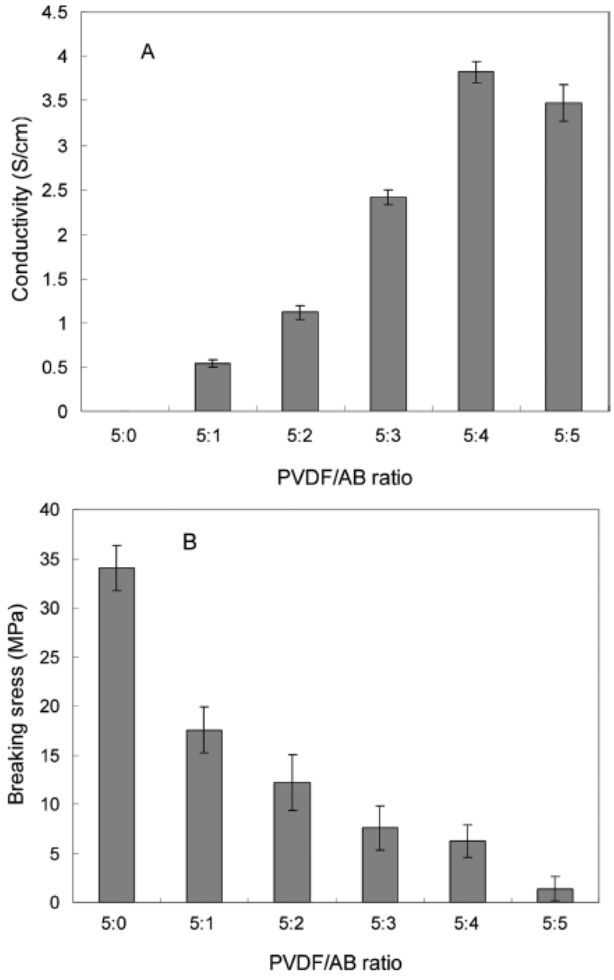

Figure 17. Electronic conductivity (A) and breaking stress (B) of the electrode composite at different PVDF/AB ratios.[11]

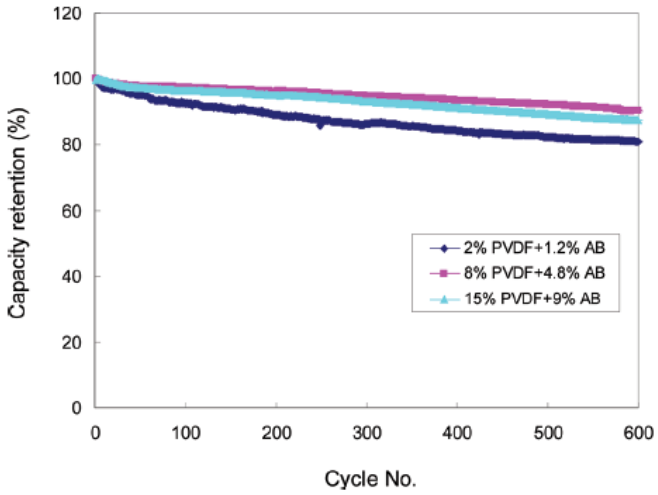

Figure 18. Cycling behavior of LiNi0.8Co0.15Al0.05O2 cathode containing different amounts of inactive materials at a 5:3 PVDF/AB ratio against MCMB anode.[11]

In anode, the binding structure of CMC thickner and SBR binder is different so that the whole electrode structure is different in order of slurry composition. CMC works as thickner to make slurry viscous so that making easy to produce the electrode. However, since the binding structure of CMC is wrapping active material particle, it can act as resistance in anode while the battery cell is in working. In 2012, Chia-Chen Li and Yu-Sheng Lin reported interaction of CMC and SBR with active material.[3] As shown in Figure 19, they suggested that SBR has higher preference with LiFePO4 than CMC thickener. However, CMC has higher preference with graphite than SBR. In that article, they experiment two different mixing sequences which are mixing CMC and SBR together and mixing CMC first and then mixing SBR last.

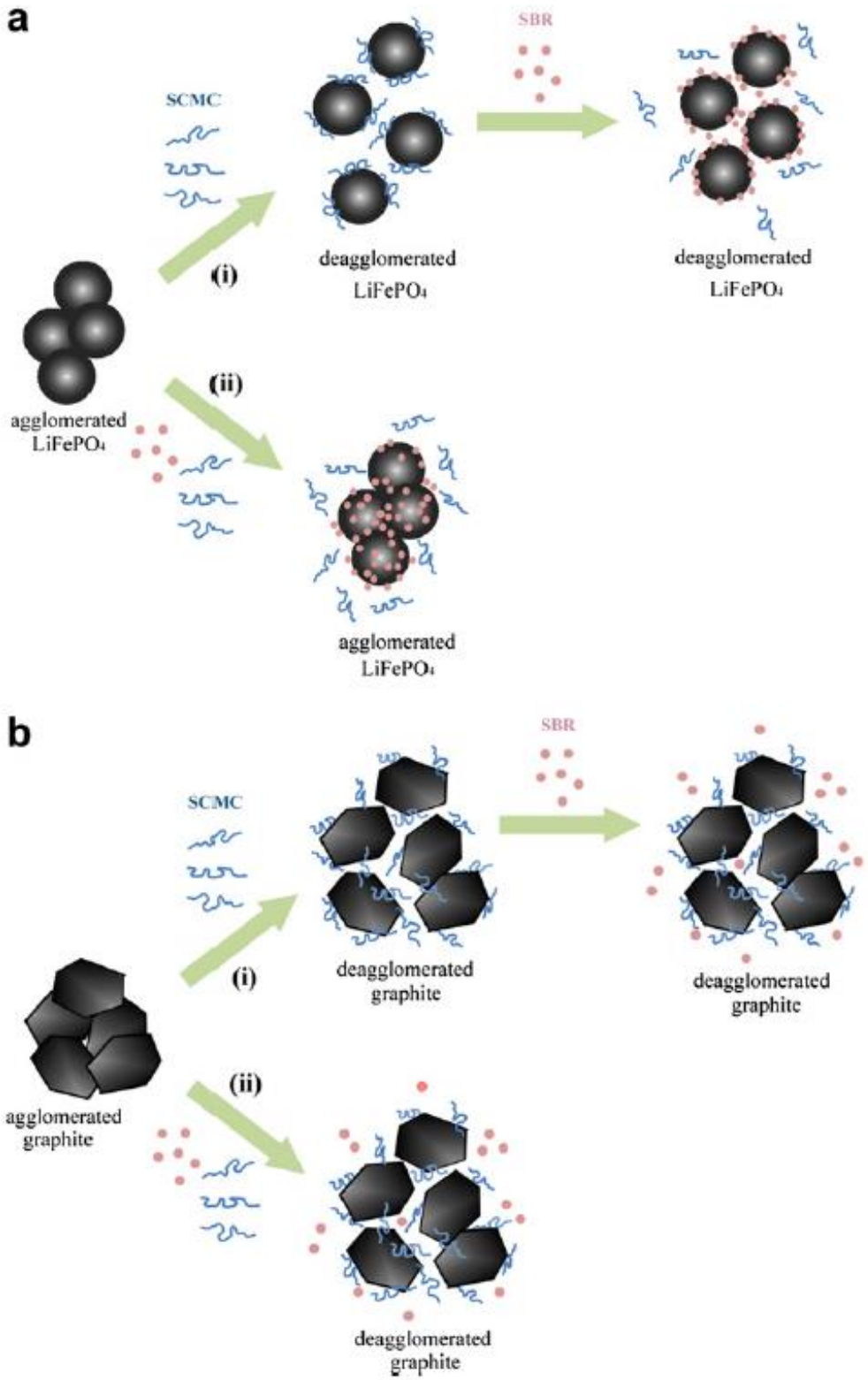

Figure 19. Diagrams showing dispersion mechanisms of (a) LiFePO4 and (b) KS6 graphite in an aqueous suspension with the presence of SBR and SCMC added via the sequence of (i) SEQ and (ii) SIM process.[3]

Recently, silicon has been researched for anode material because of its high gravimetric capacity. However, since silicon experience high volume expansion during lithium insertion, research for polymeric binder of silicon anode is being more important. Various attempts to relieve volume expansion of silicon anode has been tried by change polymeric binder. CMC shows better cycling performance compared to PVDF when use silicon graphite composite.[29] Researches to use a new kind of binder material have been existed. Electrochemically active polyamide imide binder has adopted for silicon anode.[30] In 2012, highly cross-linked polymeric binder were reported for high performance silicon anode.[31]

Those previous researches suggest the effect of binder in the electrode composite. However, to commercialize the battery, the total ratio of binder and conducting agent could not exceed 5 to 10% of total slurry since the high content of inactive material results the lower energy density of the cell. In this article, the conductive and resistive electrode component in both cathode and anode will be discussed. In cathode, the conducting agent and the PVDF binder compete the conductivity and resistivity.

The object of this research is the confirmation of the effect of inactive parts in the lithium ion battery electrode. The electrode physical property and electrochemical performance of the cell can be different depending on binder and conducting agents even though active material and its ratio is same. If it is possible to confirm the role of inactive materials in electrode composite, it would be much easier to maximize the performance of the cell without developing active material.

Ⅱ. Experimental Method

2.1. Electrode and cell manufacturing

The active material of anode and cathode were S360 graphite and NCM622 (L&F Co., Ltd.). S360 graphite was mixed with the total ratio of 2.6% binder. Experiments were done with three different ratio; 0.6% CMC with 2% SBR, 1.2% CMC with 1.4% SBR, 2% CMC with 0.6% SBR. The active material ratio were all maintained equally and each of the three samples were mixed in homogenizer with 12000rpm for 1 hour. Mixed slurry was coated in 10mg/cm^2 loading on the 18um thick Cu substrate and were dried in the 80ºC oven for 1 hour. Dried electrodes were roll pressed to 1.6g/cc and vacuum-dried in the 110ºC oven for 8 hours. NCM622 was mixed with PVDF binder and two different conducting agents. KF9300 (Kureha) was used as binder and Super P and Ketjen Black were used as conducting agent. Slurry was mixed with the two different ratio of binder and the conducting agent; 2% binder with 2% conducting agent and 2.5% binder with 1.5% conducting agent. The active material ratio was fixed as 96% for all samples. The cathode slurries were mixed in homogenizer with 10000rpm for 1.5 hour. Slurry was coated on 30um Al substrate in 17.5mg/cm^2 loading level and dried in the 110ºC oven for 1 hour. After roll pressed to 3.3g/cc, electrodes were vacuum-dried in the 110ºC oven for 8 hours.

The cathode samples were tested in 2032 coin half-cell and the anode samples were tested in pouch full-cell. Coin half-cell was assembled in the glove box and pouch full-cell was assembled in the dry room. Electrode was punched in 14pi-size for coin half-cell. For pouch full-cell, cathode was punched in 20mm*25mm size and anode was punched in 22mm*27mm size. The electrolyte used for both coin half-cell and full-cell is 1.15M $LiPF_6$ dissolved in mixed organic solvents, consisting ethylene carbonate (EC), ethyl methyl carbonate (EMC), Diethyl carbonate (DEC) in the volume ratio of 3:6:1

Figure 20. The SEM image of Graphite S360(left) and NCM622(right).

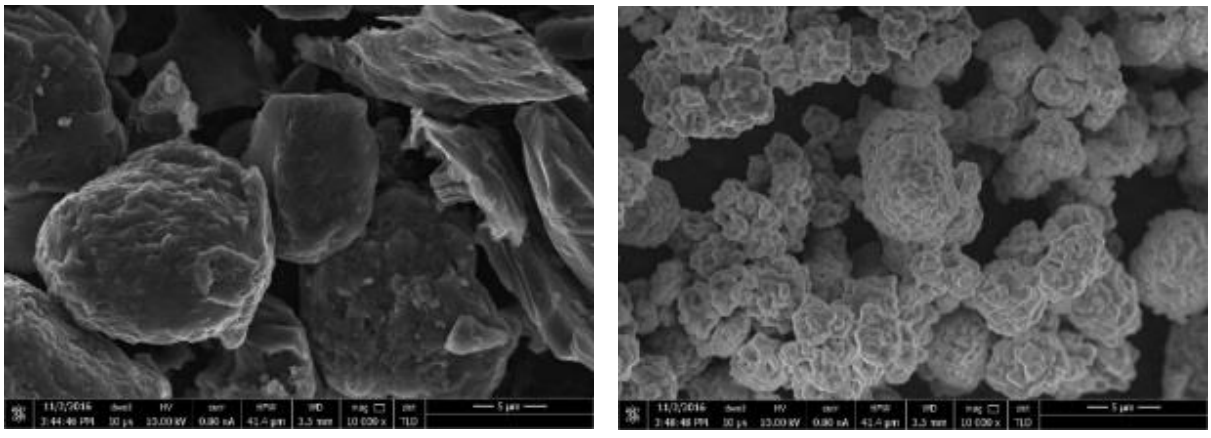

with additives of 1% VC and 2% PS. (PANAX ETEC Co. Ltd., Korea)

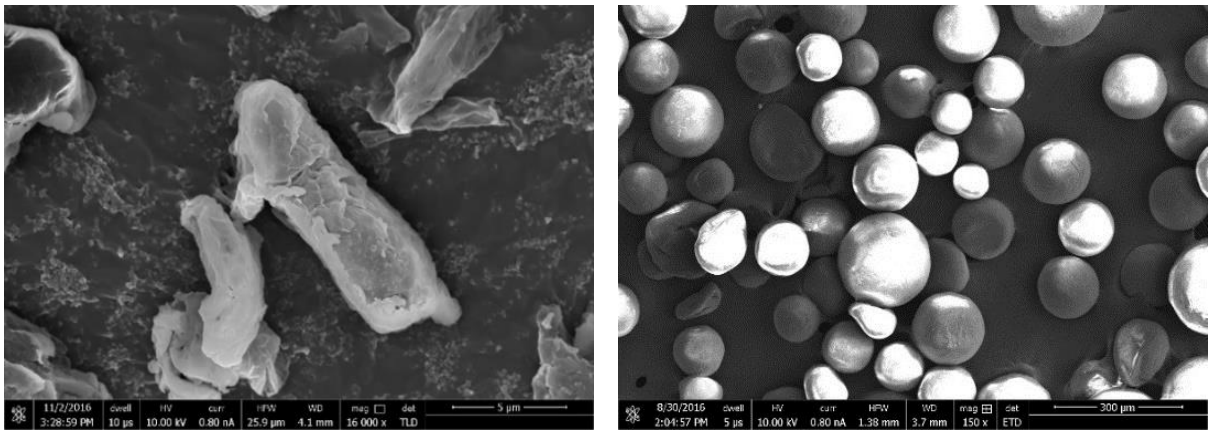

Figure 21. The SEM image of CMC(left) and PVDF(right).

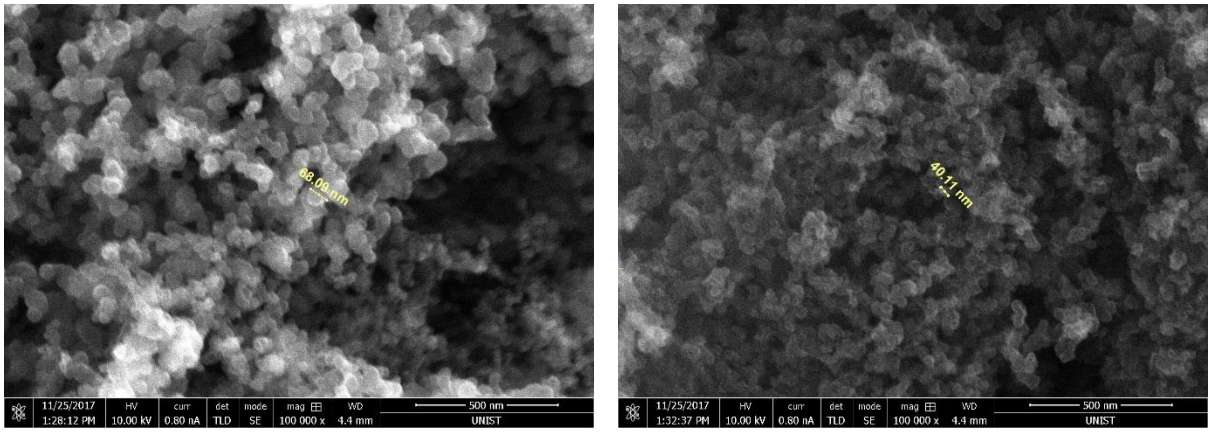

Figure 22. The SEM image of Super P(left) and Ketjen Black(right) conductive agent.

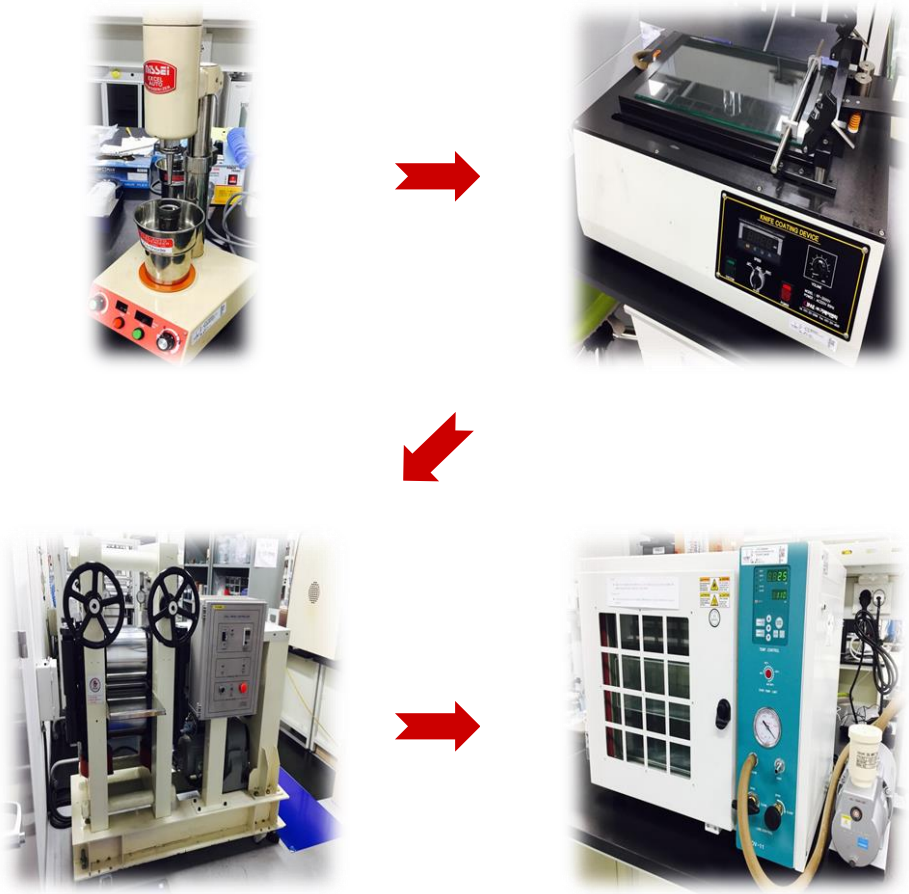

Figure 23. The Electrode manufacturing process consists of mixing, coating, pressing and vacuum drying.

2.2. Physical characterization

Scanning Electronic Microscopy (SEM, S-4800, HITACHI) was used to determine slurry dispersion and electrode condition. Freeze dryer was used to obtain the SEM image of cathode and anode binder solution and slurry. Since binder solution and slurry are colloid form solution, freeze dried samples of them were observed by SEM. Anode binder solution and slurry were freeze-dried for 5 days. Cathode binder solution and slurry were freeze-dried for 1 week at the temperature of -88^{o}C and pressure of 5mTorr.

The cross-section electrode images were obtained by using Ion milling (IM4000, HITACHI). Ion milling was done by Argon ion for 2 hours. Ion beam current is 107μA and argon gas flow of 0.15cm^{3}/min.

The electrode adhesion strength test was done by the adhesion strength tester (DS2-50N, IMADA). Testing electrode length was 30mm and width was 15mm. Desorption speed was 50mm/min.

Figure 24. Scanning Electronic Microscopy(left) and Ion milling(right).

2.3. Electrochemical characterization

Charge and discharge cycles were done by TOYO TOSCAT. The cathode half cell was charged from 3V to 4.3V. 1C rate charge and discharge were done for 50 cycles. 3C rate charge and 1C rate discharge were done for 50 cycles. Full cell was charged from 2.8V to 4.2V. 1C charge and discharge were done for 50 cycles. 3C charge and 1C discharge were done for 20 cycles. Charge cut off was 1/50C. Electrochemical Impedance Spectroscopy (EIS) was measured by Biologic EC-Lab. For half cell, EIS measurement was done at 4.28V. Frequency sweep from 1MHz to 10mHz and voltage range was 10mV. Electrode electrical conductivity was measured by 4 probe measurement using Resistivity meter (DASOLENG CO.,LTD, Korea). Cathode and anode slurry were casted on Mylar film to exclude Al or Cu foil effect.

Ⅲ. Results and Discussions

3.1. Anode

3.1.1. Anode binder and slurry freeze dry

CMC thickner and SBR binder showed different structure when observing them by SEM after freeze dry. Figure 25 shows SBR has point-connected structure and CMC has gum-like structure. The figure 26 below shows the freeze-dried slurry of three different samples. The high SBR sample has point-binding and the high CMC sample has face binding. When mixed in slurry, CMC covering graphite particles together which looks like face-binding. SBR exists as small grain and connects active material particles. In Figure 26 f), it is clearly seen that CMC thickner covering graphite particle.

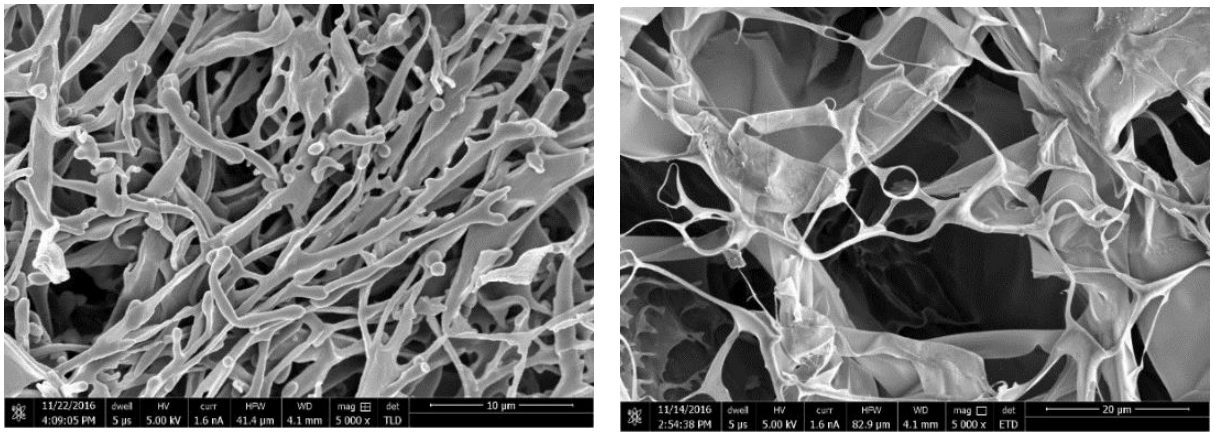

Figure 25. The SEM image of freeze-dried SBR binder (left) and CMC thickener (right).

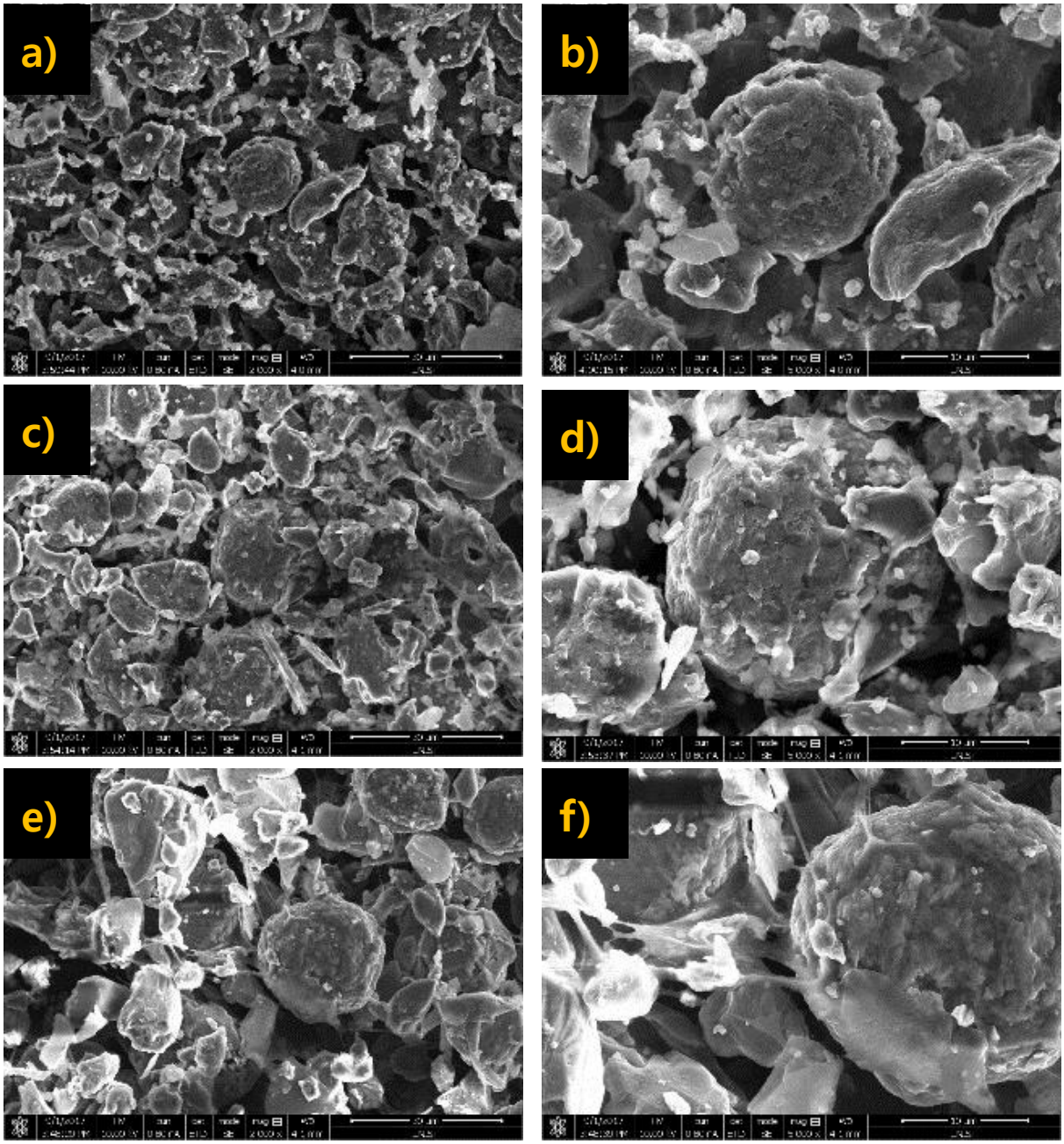

Figure 26. The SEM image of freeze-dried slurry of a) High SBR low CMC ratio c) middle SBR and CMC ratio e) low SBR high CMC ratio and expanded SEM image of freeze-dried slurry of b)High SBR low CMC ratio d) middle SBR and CMC ratio f) low SBR high CMC ratio.

3.1.2. Anode Physical property

Anode test electrodes showed different physical properties in adhesion test. Electrode with the high CMC ratio shows the highest average binding strength of 5.029 gf/15mm and maximum binding strength of 5.4 gf/15mm. High SBR, low CMC ratio electrode showed the lowest average binding strength of 1.8 gf/15mm and maximum binding strength of 2.933 gf/15mm. Since CMC has the face binding structure which covers active material particles, it has better binding ability compare to SBR so that the high CMC ratio electrode has higher binding force than the low CMC ratio electrode. From this result, it is possible to predict that the fatigue stress of the high CMC ratio electrode would be higher than the low CMC ratio electrode.

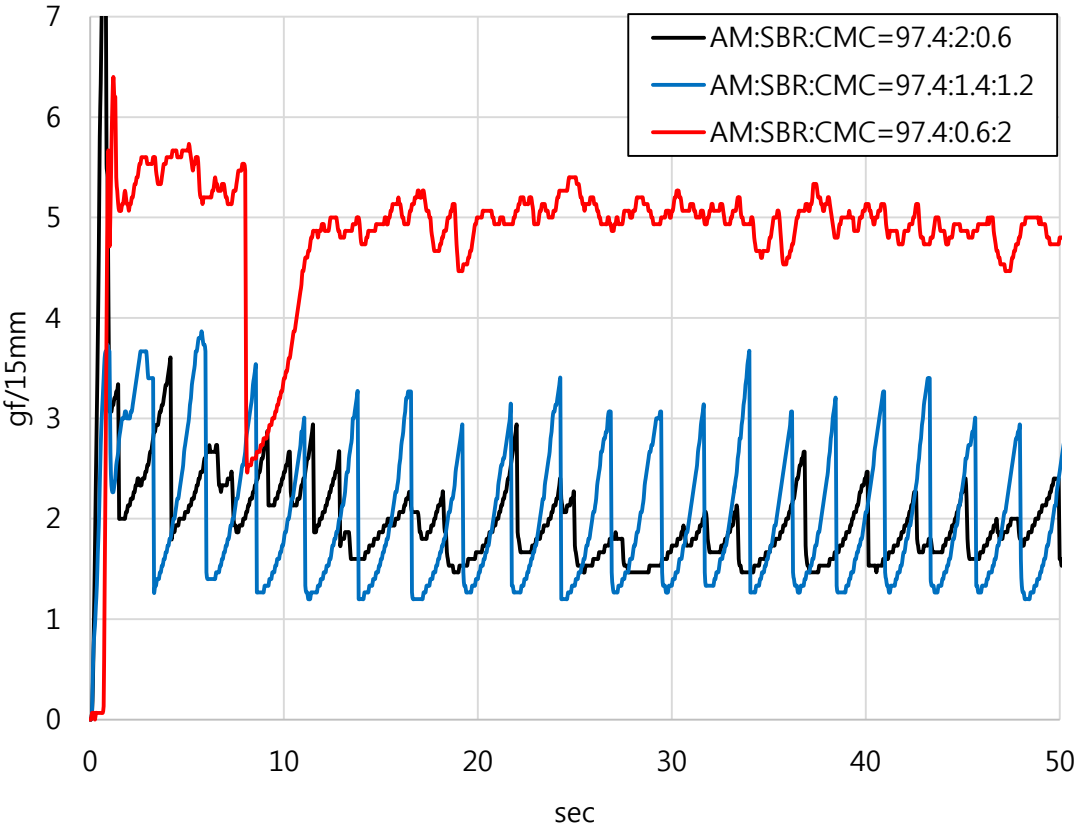

Figure 27. The Adhesion test result of Anode electrodes.

Table 1. Adhesion test result of Anode electrodes.

30 - 50sec (gf/15mm)			
AM:SBR:CMC ratio	97.4:2:0.6	97.4:1.4:1.2	97.4:0.6:2
average load	1.800	1.933	5.029
maximum load	2.933	3.666	5.400

3.1.3. Anode Electrochemical property

Figure 28 is the formation profile of three different full cells. The full cell of each sample shows different initial capacity. Electrode with high CMC ratio shows lower initial capacity compared to the high SBR ratio electrode when their active material ratio and weight is all same. The full cell with the high CMC ratio anode shows the initial capacity of 13.5mAh. The full cells which have the middle and the low CMC ratio anode shows the initial capacity of 13.8mAh and 14.1mAh each. The voltage profile during charge state, the red line cell which is the high CMC ratio cell has higher potential compare to other two cells. Also, during discharge state, the red line has the lowest potential compare to other two samples. These results show that electrode with high CMC ratio anode has higher overpotential during charge and discharge at the initial cycle.

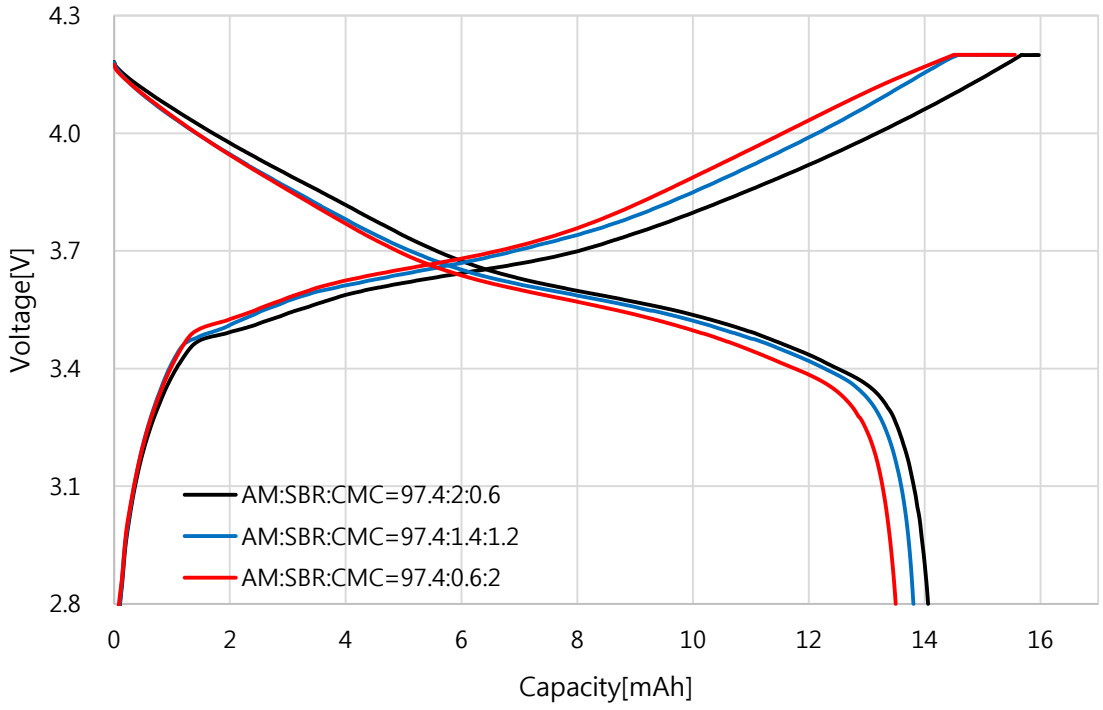

Figure 28. Formation profile of full-cell.

However, the cycle retention of high CMC ratio electrode was better than the high SBR ratio electrode when charging for 3C rate. After 20 cycles, high CMC ratio electrode showed 62% retention and high SBR ratio electrode showed 42% retention. Voltage profile of the 1st, 10th and 20th cycle shows how overpotential affects in charge and discharge processes. At the 1st cycle of 3C rate charge, the high CMC ratio and middle CMC ratio cell shows similar charge voltage. The constant current charging held for 13 to 16 minutes for three samples. However, at the 10th cycle of 3C rate charge, the charge voltage

of the high CMC ratio cell is much lower than the high SBR ratio cell. Constant current charging for high CMC ratio cell held for more than 8 minutes but for high SBR ratio cell, it held for about 4 minutes. The gap between them being more dramatic at 20th cycle. Constant current charging for high CMC ratio cell held for more than 6 minutes but for the high SBR ratio cell, it held for less than 2 minutes. At 20th cycle, the time ratio of CC and CV charging for high CMC ratio cell is about 1:3. However, CC and CV charging time ratio for high SBR ratio cell is about 1:12.

When charging for 1C rate, the charge voltage gap between samples is much lower than 3C rate. The charge voltage profile of 1st, 20th, 50th cycles suggest the high CMC ratio cell has lower charge voltage, but the difference is much lower than 3C rate charging. Nonetheless, the cycle retention tendency at 50th cycle is same to 3C rate charging. After 50 cycles, the high CMC ratio electrode shows 90% retention. The middle CMC ratio electrode and the low CMC ratio electrode show 89% and 85.7% respectively. Both 3C rate charge rate capability test and 1C rate cycle life test shows that the high CMC ratio electrode has better cycle retention compare to the low CMC ratio electrode. These results are also co-related to the adhesion test result which shows the mechanical binding ability of three electrodes. Electrode which has the better mechanical binding ability has higher fatigue stress.

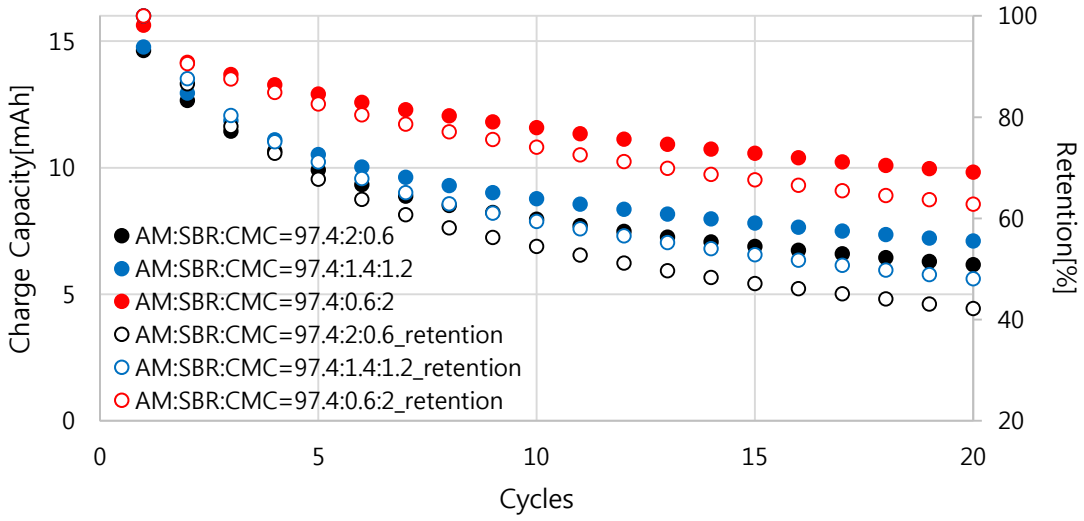

Figure 29. 3C rate cycle retention of full-cell

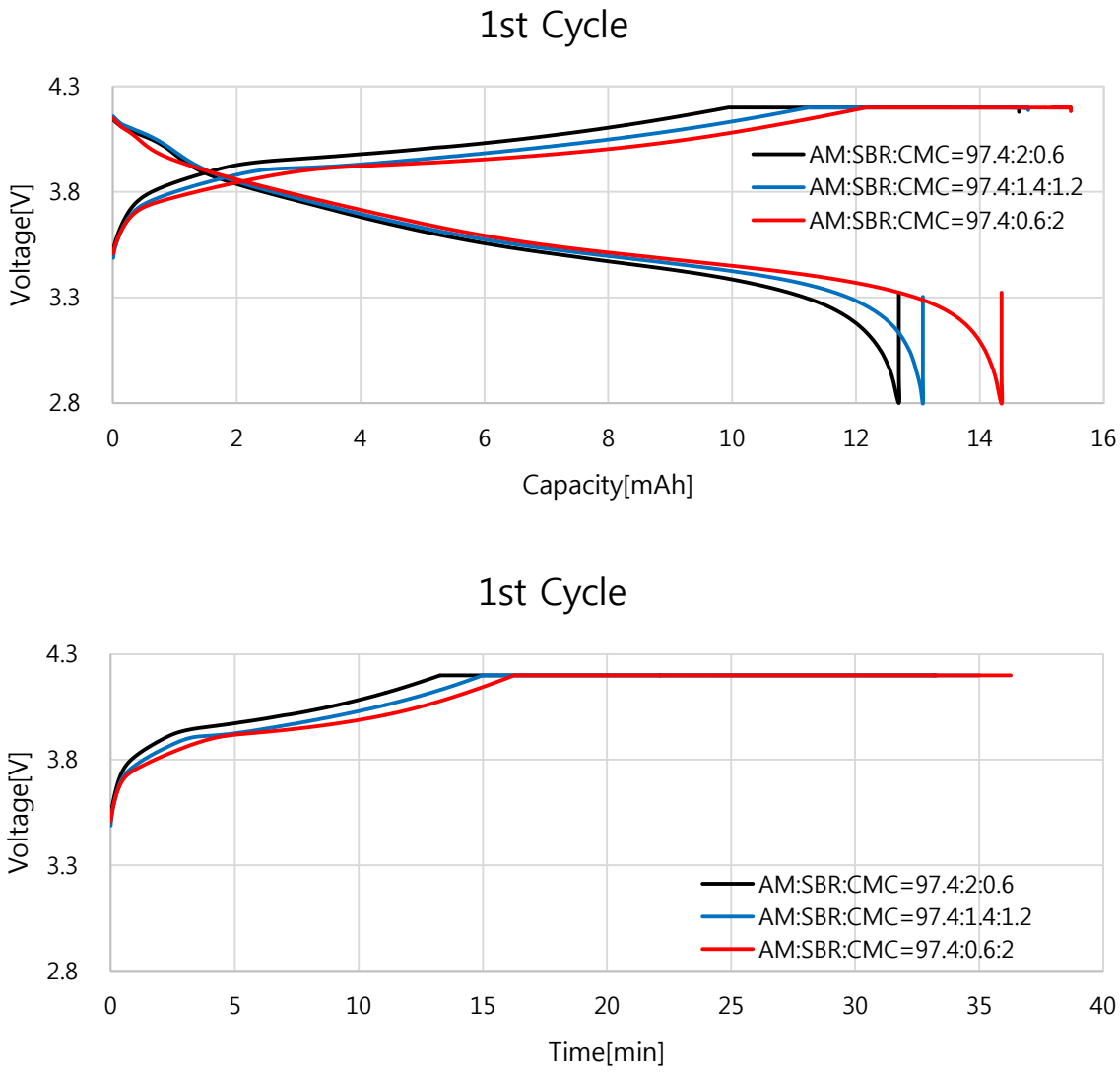

Figure 30. Voltage profile of 1st cycle and time plot of charge process at 3C rate charging.

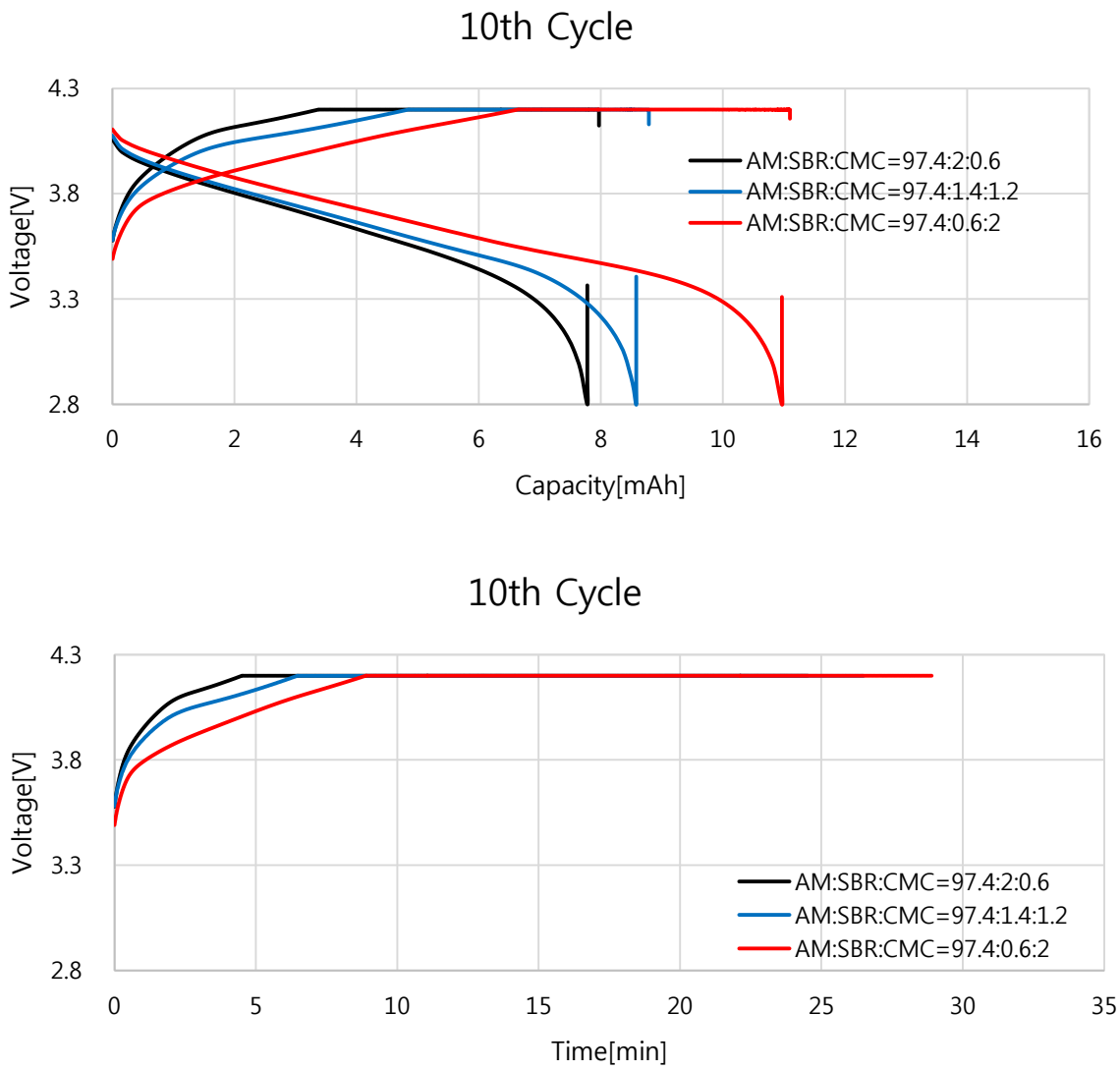

Figure 31. Voltage profile of 10th cycle and time plot of charge process at 3C rate charging.

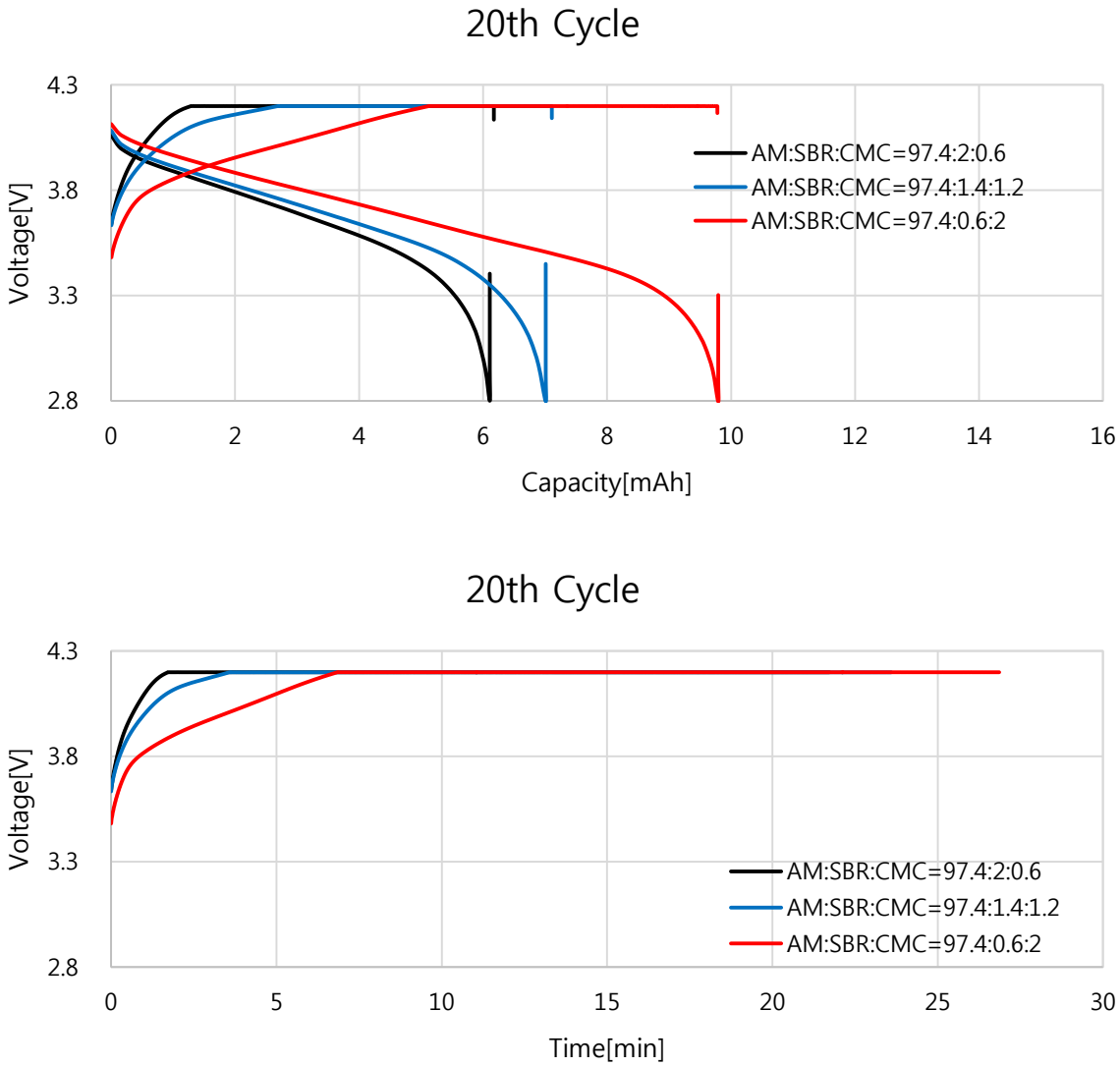

Figure 32. Voltage profile of 20th cycle and time plot of charge process at 3C rate charging.

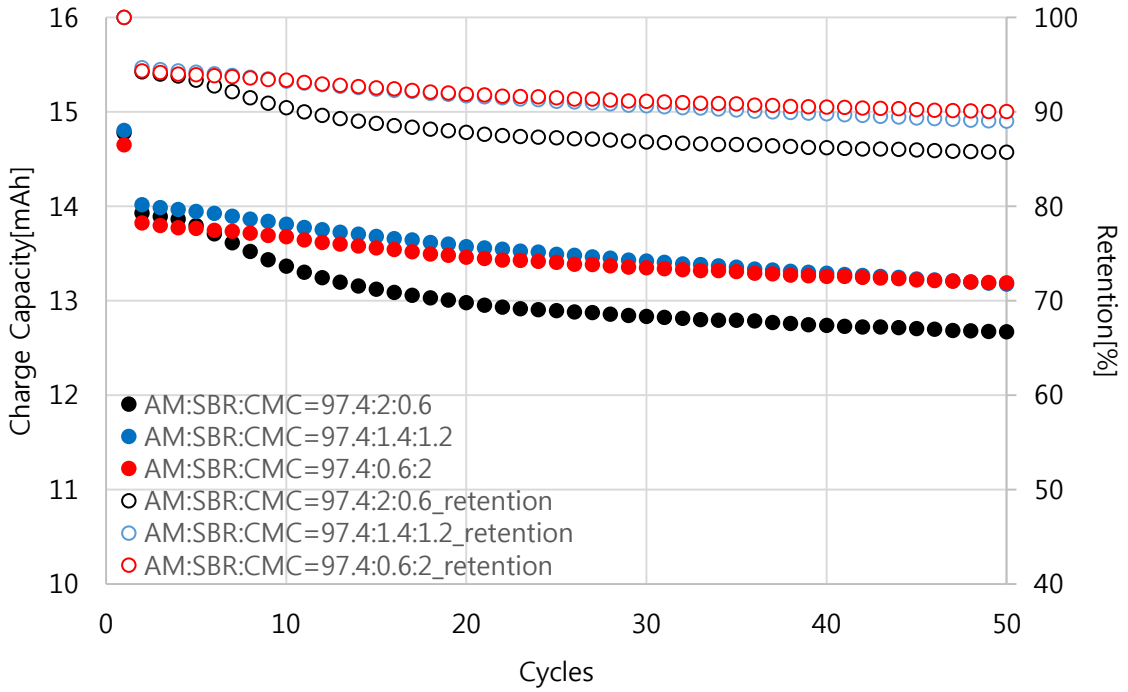

Figure 33. 1C rate cycle retention of full-cell.

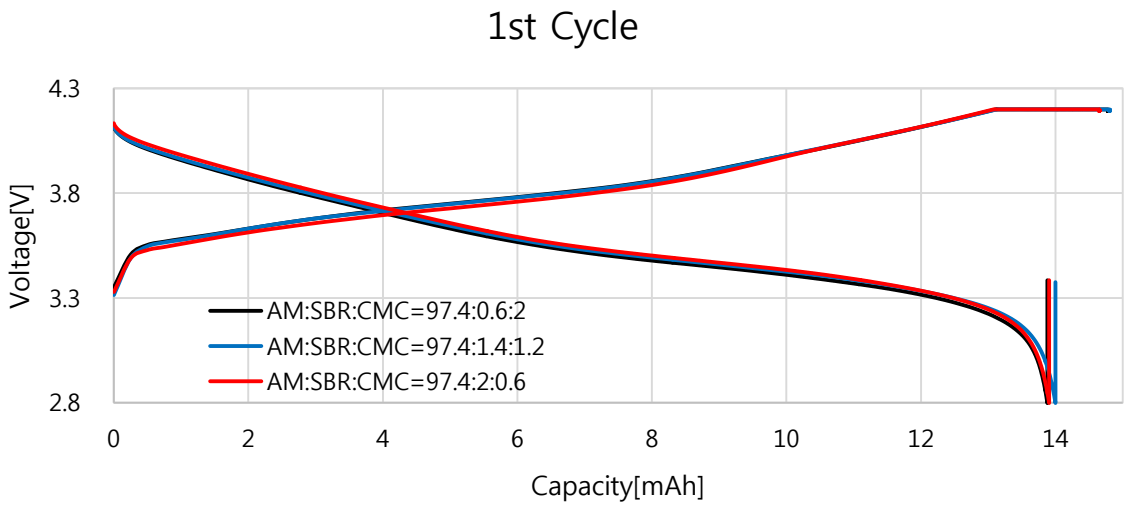

Figure 34. Voltage profile of 1st cycle at 1C rate charging.

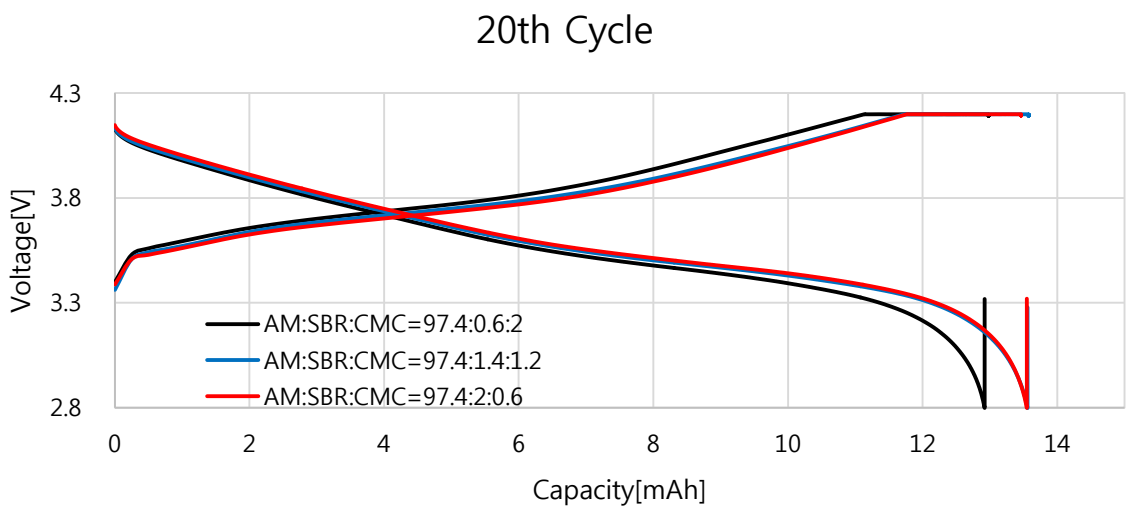

Figure 35. Voltage profile of 20th cycle at 1C rate charging.

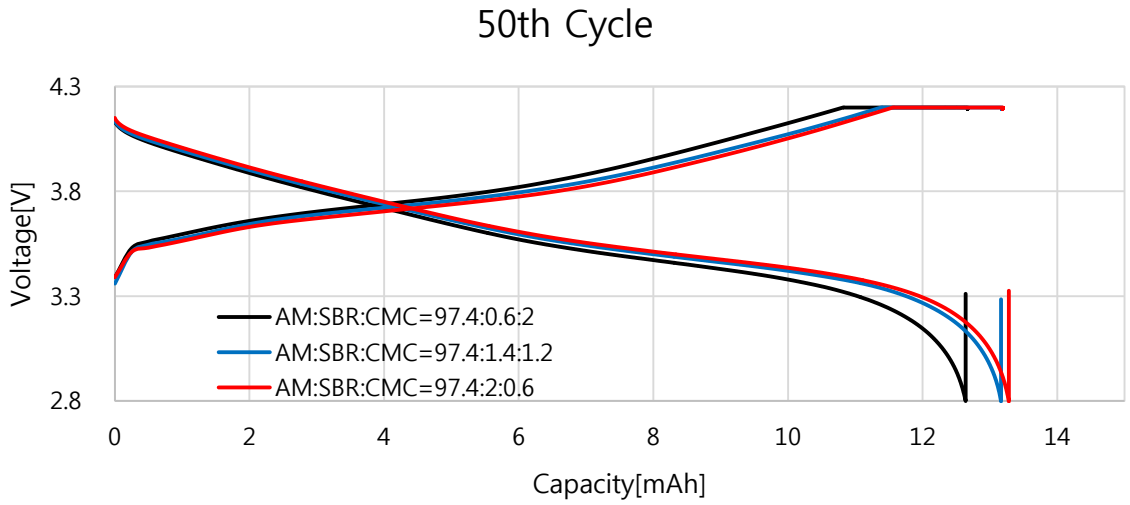

Figure 36. Voltage profile of 50th cycle at 1C rate charging.

In electrode electrical conductivity test, the electrode with the high CMC ratio showed the lower electrical conductivity of 8.30 S/cm than the electrode with the low CMC ratio which showed 15.06 S/cm. Electrode with the middle CMC ratio which has 1.2% of CMC and 1.4% of SBR showed the electrical conductivity of 9.21 S/cm which is higher than the electrode electrical conductivity of the low CMC ratio electrode. Since there is no conductive agent in composite, this result proves that binder plays the role of resistance in the electrode composite.

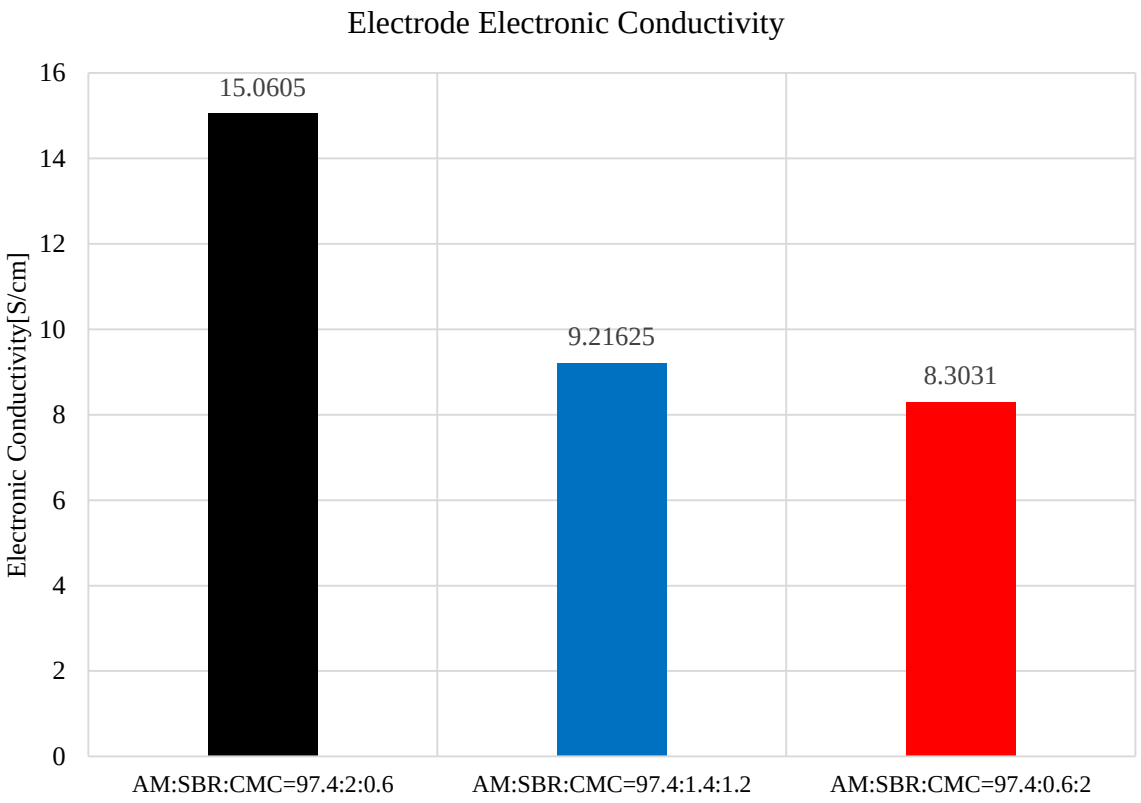

Figure 37. The Electronic conductivity of anode composite.

Table 2. Electronic conductivity of anode composite.

	AM:SBR:CMC 97.4:2:0.6	AM:SBR:CMC 97.4:1.4:1.2	AM:SBR:CMC 97.4:0.6:2
Electronic Conductivity(S/cm)	15.0605	9.21625	8.3031

Since the wettability difference of CMC and SBR can affect rate capability of anode, the contact angle of anode samples were measured. When measuring the exterior angle of electrode surface, the average contact angle of the high CMC ratio electrode was 159.8^{o} and standard deviation was 1.89^{o}. The average contact angle of the low CMC ratio electrode was 161.2^{o} and standard deviation was 2.2^{o}. The ANOVA test was done to check those numerical values' statistical differences. The null hypothesis of the test is, "the three samples are not differ from one another." For the analysis of variance, the variance of each samples are assumed to same statistically. At the ANOVA test, as shown in table 3, the result P-value was 0.000 which means the mean of three samples are not same. Therefore, the null hypothesis is rejected. Among three samples, 1.2% CMC with 1.4% SBR ratio electrode showed lower average contact angle of 155.2 ^{o} with standard deviation of 1.65^{o}. There was no significant difference

between the 2% CMC ratio electrode and the 0.6% CMC ratio electrode. The reason of this phenomenon is not defined yet. In other words, the effect of wettability difference of CMC and SBR is not clear in contact angle measurement when the binder ratio is less than 2.6%.

Table 3. The contact angle of electrolyte with anode electrodes.

trial	CMC 0.6% SBR 2%	CMC 1.2% SBR 1.4%	CMC 2% SBR 0.6%
1	167.629	155.748	159.416
2	162.707	153.376	159.002
3	159.089	156.216	161.869
4	160.103	155.676	160.031
5	159.086	152.957	159.175
6	161.951	155.33	161.103
7	158.799	153.729	161.098
8	160.598	154.868	157.48
9	161.459	157.996	160.839
10	161.498	156.923	155.739
11	163.779	157.571	158.726
12	161.943	156.254	161.308
13	159.773	151.849	161.37
14	159.178	155.569	161.9
15	160.618	154.958	162.868
16	159.499	155.074	159.162
17	162.059		157.991
18			160.104
19			156.801
AVERAGE	161.16282	155.25588	159.7885
STDEV	2.205866	1.6556344	1.890382

	DF	Adj SS	Adj MS	F-value	P-value
Factor	**2**	**314.4**	**157.176**	**42.02**	**0.000**
Error	**49**	**183.3**	**3.741**		
Total	**51**	**497.6**			

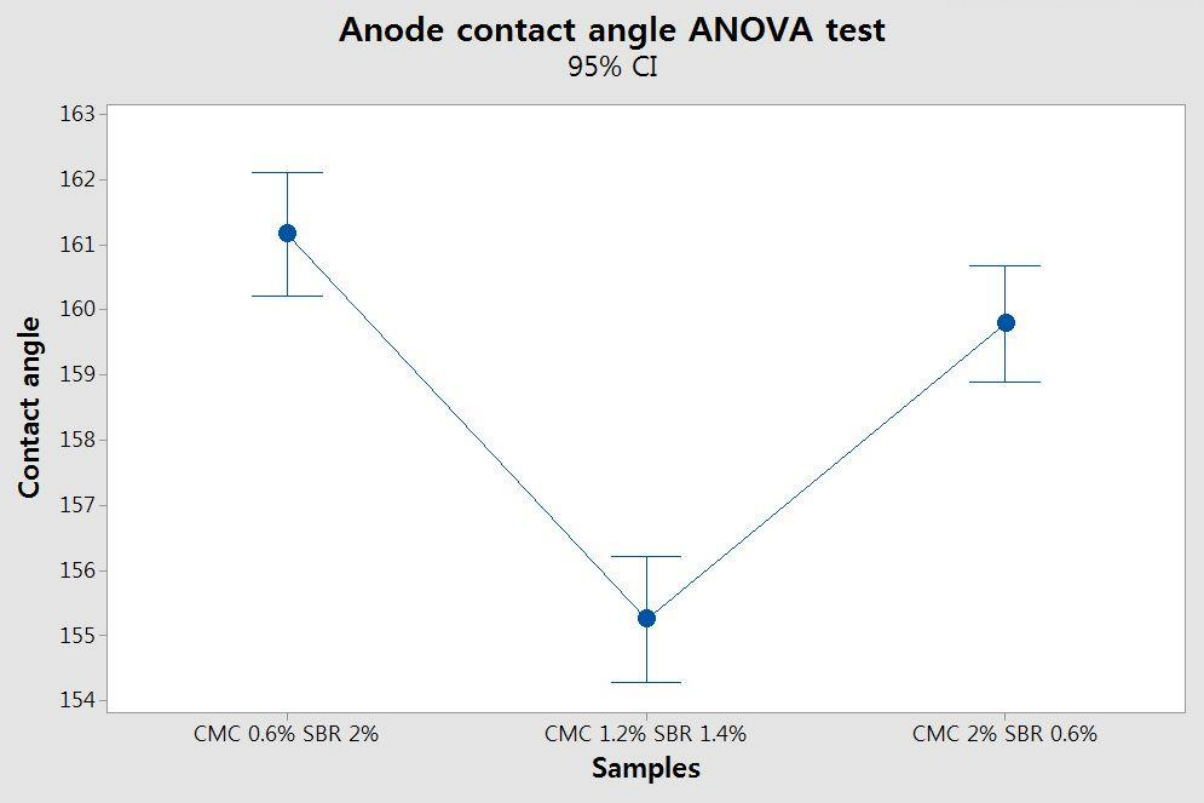

Figure 51. ANOVA test result of three different anode samples. The 1.2% CMC with 1.4% SBR ratio electrode shows lower contact angle among three samples but the difference between high CMC electrode and low CMC electrode is not significant.

From those experiments, it was possible to confirm that binder which has face binding structure can resist electronic conduction between active material particles. However, since the role of binder is mechanical binding of active material on the substrate, it is unavoidable to use face binding structured binder in the electrode composite. If the anode uses silicon or silicon graphite composite, usage of a face binding structured binder would be essential. Therefore, optimizing the ratio of face binding and point binding structured binders is needed. Also, using polymeric binder which has a longer chain would be helpful to lower the ratio of face binding structured binder and enhance mechanical binding strength simultaneously. To confirm the effect of CMC more clearly, it is necessary to check 2.6% CMC ratio electrode without SBR contents. Future work with the electrode which has only CMC binder will confirm the effect of the face binding structured binder in the anode composite more clearly.

3.2. Cathode

3.2.1. Cathode binder and slurry freeze dry

Cathode binder PVDF has similar binding structure with CMC of the anode which covers active material particles. When PVDF binder and carbon conducting agent mixed together, the conducting agent locates in binder grain and help electronic conduction in cathode. Slurry freeze-dried image shows PVDF binder mixed with conducting agent covering NCM particles. When the binder ratio is 2.5% and super P ratio is 1.5%, it is possible to observe poor conducting network compare to 2% ratio of binder and super P. In case of Ketjen black conducting agent, the slurry freeze-dried image shows the well dispersed conducting agent compare to slurry with the super P conducting agent as shown in figure 38.

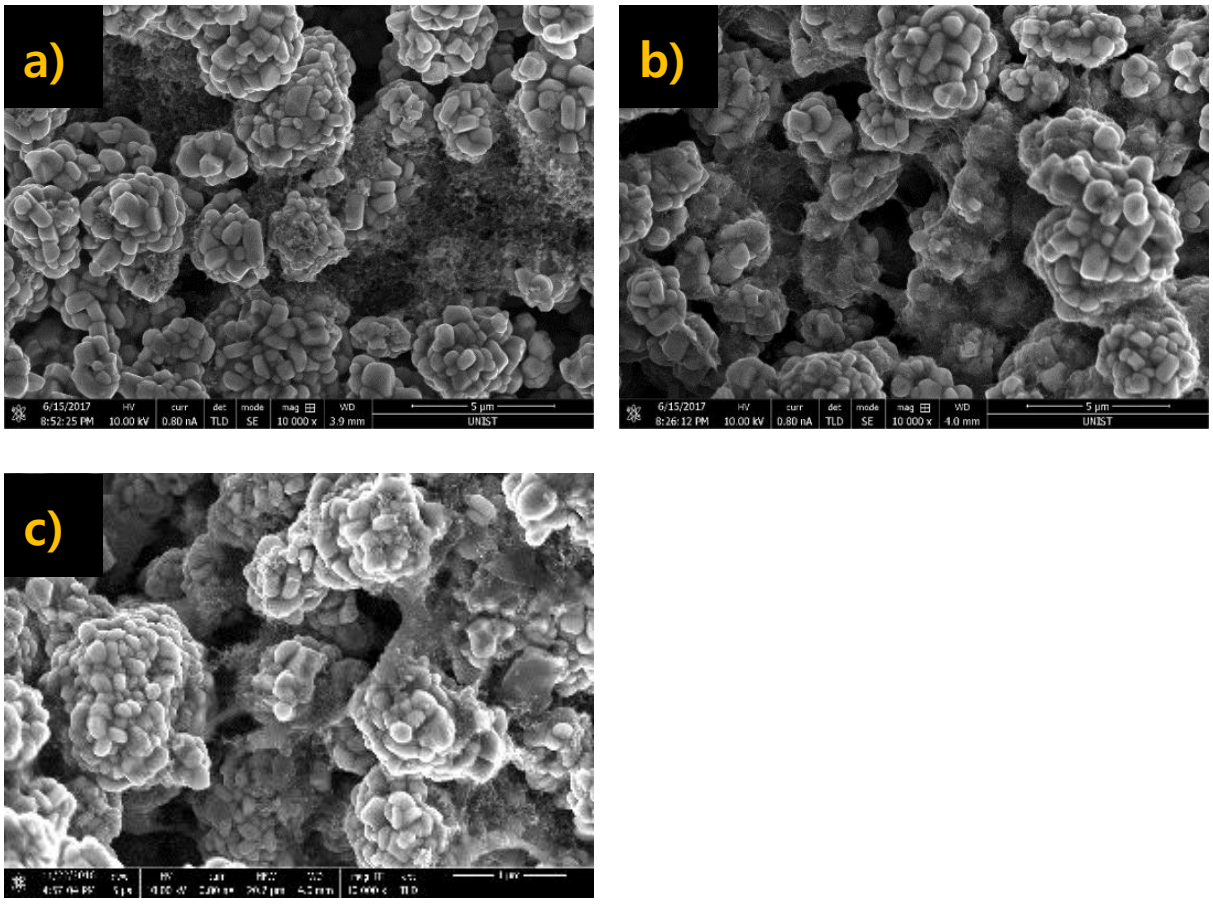

Figure 38. The SEM image of freeze-dried slurry with a) Super P conducting agent (2%), b) Ketjen Black conducting agent (2%), c) Super P conducting agent (1.5%).

3.2.2. Cathode Physical property

Electrode with the high PVDF ratio electrode showed higher mechanical strength. It has the same tendency compare to the anode case. Electrode which uses Ketjen black as conducting agent showed lower mechanical strength than the electrode which uses super P as conducting agent.

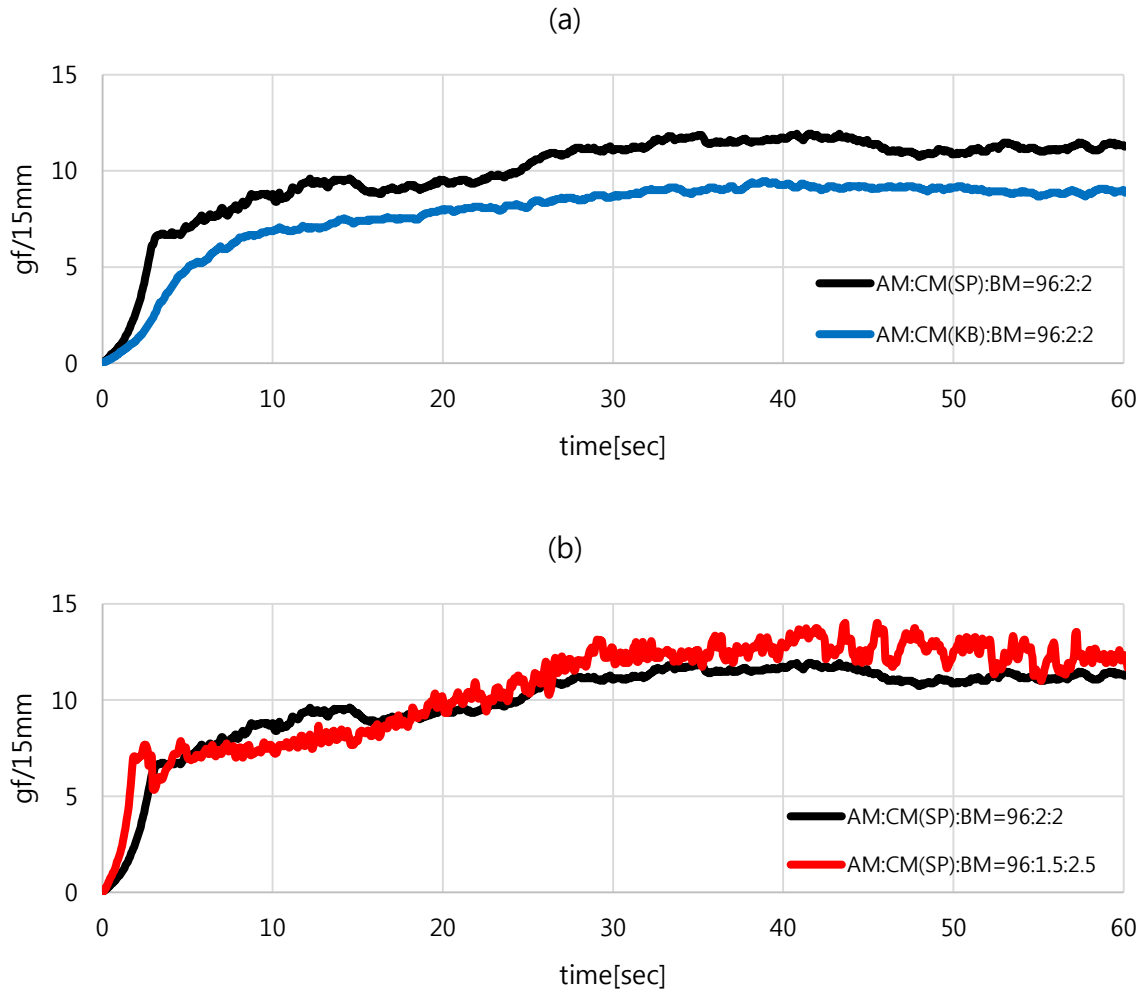

Figure 39. The Adhesion test result of cathode (a) comparing difference according to type of conductive agent, (b) comparing difference according to binder and conductive agent ratio.

Table 4. Adhesion test result of cathode electrodes.

	30 - 50sec (gf/15mm)		
AM:CM:BM ratio	96:2:2(SP)	96:1.5:2.5(SP)	96:2:2(KB)
average load	11.446	12.670	9.096
maximum load	11.933	14.000	9.466

3.2.3. Cathode Electrochemical property

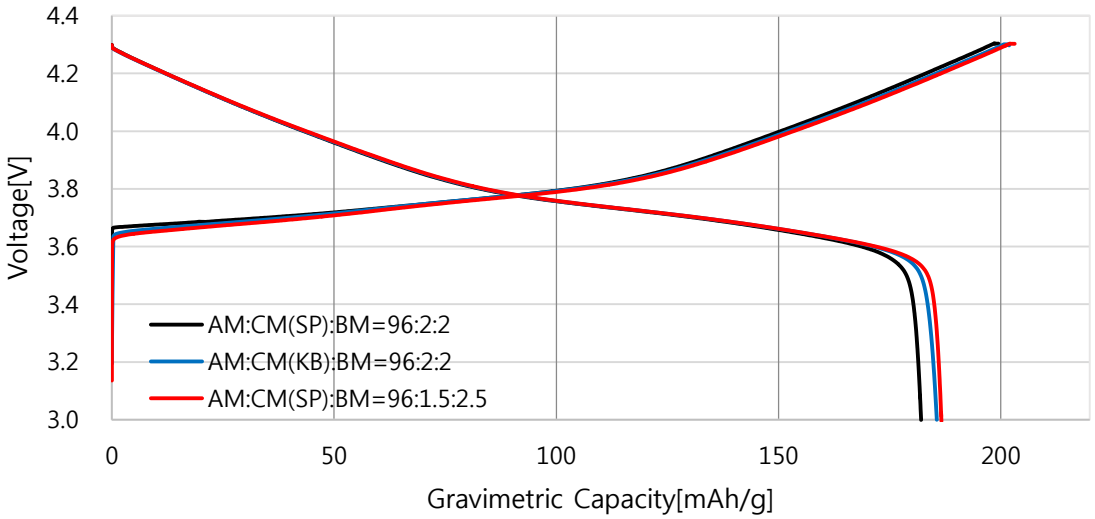

Figure 40. Formation voltage profile of cathode.

The formation voltage profile of three samples are similar to each other. However, the difference between samples in cycle retention at 1C and 3C rate charging is significant. Cell with higher PVDF ratio electrode showed poor cycle at 1C and 3C rate charging cycle retention. In 1C rate cycles, 2.5% PVDF ratio electrode half-cell showed 44% retention which is much lower than 2% PVDF ratio electrode which showed 60.2% retention after 50 cycles. The 3C charge and 1C discharge cycle retention also shows similar result. 2.5% PVDF ratio electrode half-cell shows 38.3% retention after 50 cycles. 2% PVDF ratio electrode half-cell shows 47.2% retention at 50 cycles. This result is not consistent with anode high CMC ratio electrode result because higher PVDF ratio accompanies the lower conducting agent ratio. When conducting agent is not sufficient, the conducting network cannot be well established so that cell performance can be deteriorated.

Voltage profile of the 1st, 20th, 50th cycle of 1C rate charging suggest high overpotential of the poor conducting network electrode. At the initial cycle, 2.5% PVDF ratio cell shows similar capacity compare to other samples, but it has high charge voltage and low discharge voltage. At the 20th cycle, the charge and discharge voltage gap between 2.5% PVDF ratio cell and 2% PVDF ratio cell expanded and at 50th cycle, the difference looks definite. Voltage profiles of 3C rate charging reveal the importance of the well-established conducting network in cathode composite. 2.5% PVDF ratio cell almost do not have the constant current charging mode at the initial cycle of 3C rate charging. At the 20th and 50th cycle of 3C rate charging, all three samples have high overpotential that they do not have CC mode charging. However, at discharge process, 2.5% PVDF ratio electrode has 0.2V to 0.4V lower discharge

voltage than other two samples.

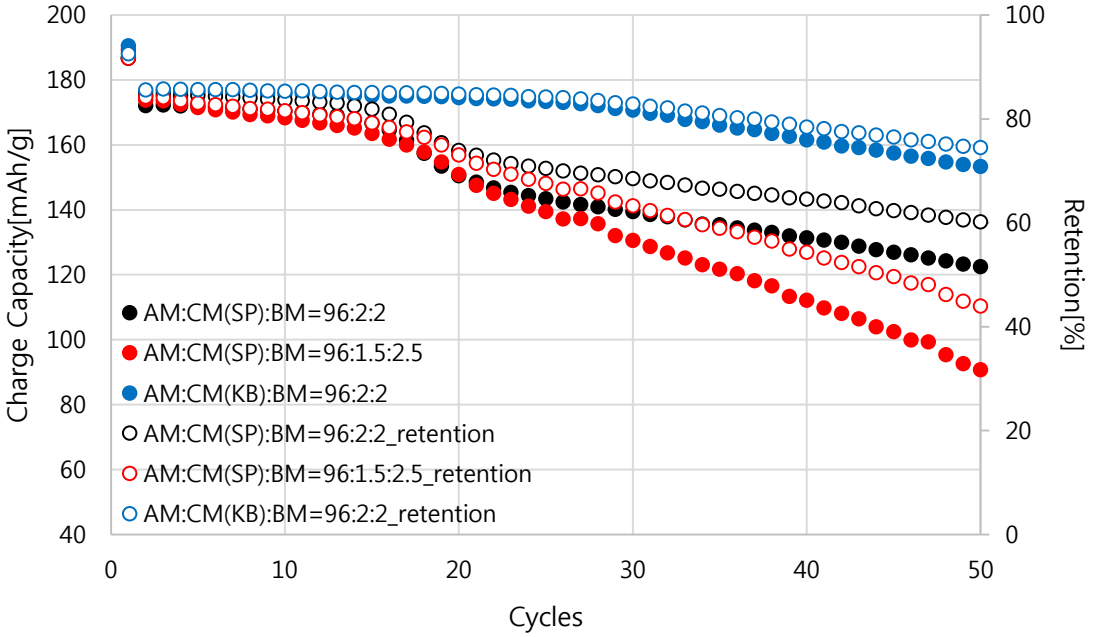

Figure 41. 1C rate cycle retention of half-cell

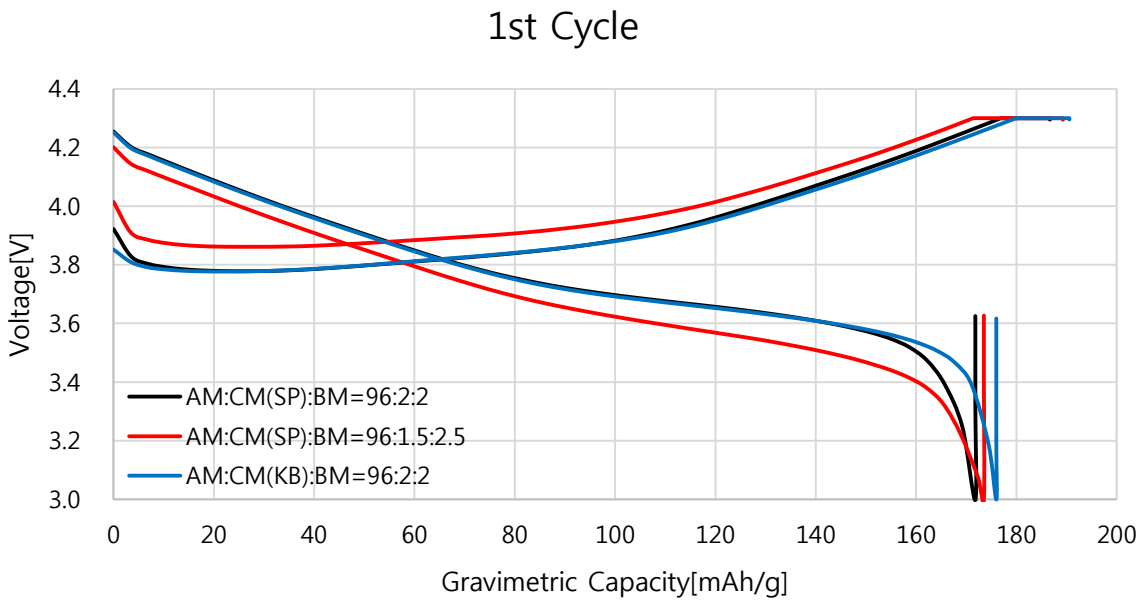

Figure 42. Voltage profile of 1st cycle at 1C rate charging.

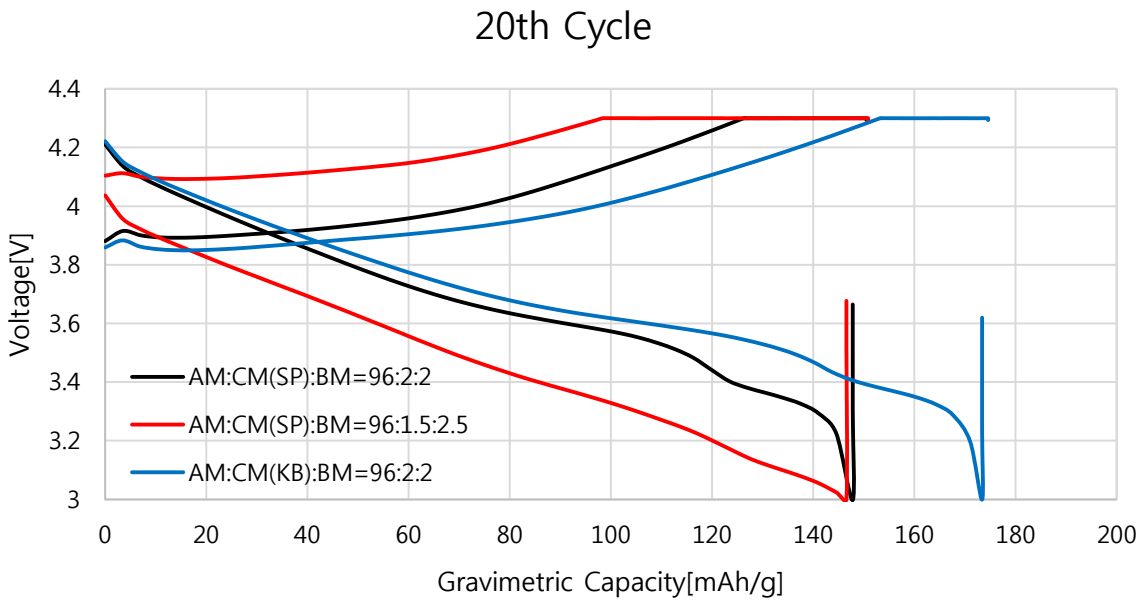

Figure 43. Voltage profile of 20th cycle at 1C rate charging.

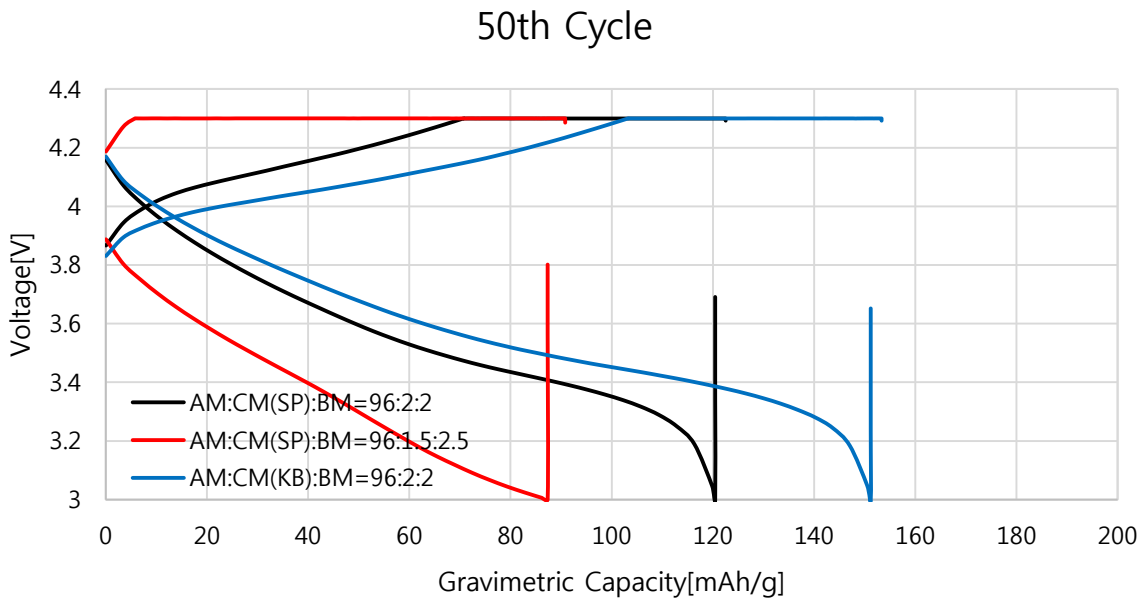

Figure 44. Voltage profile of 50th cycle at 1C rate charging.

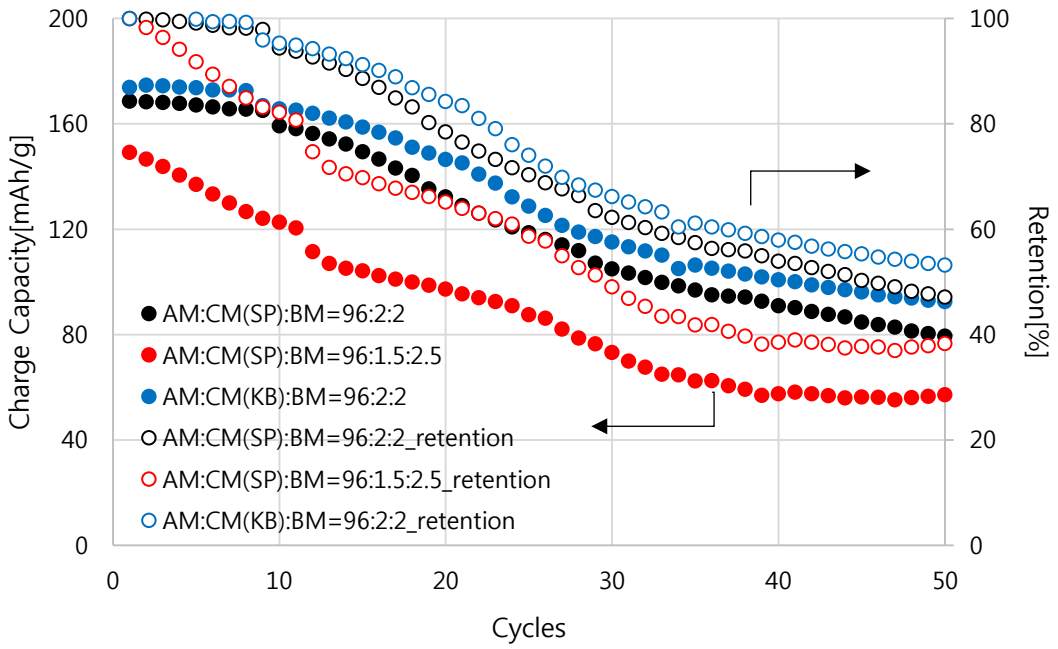

Figure 45. 3C charge 1C discharge cycle retention of half-cell.

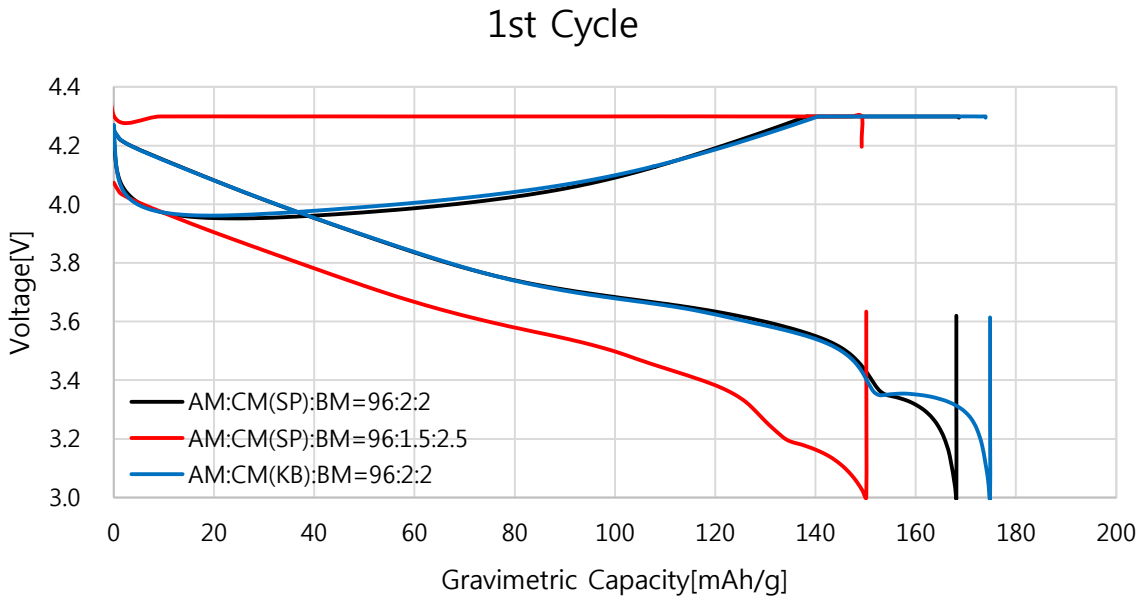

Figure 46. Voltage profile of 1st cycle at 3C rate charging.

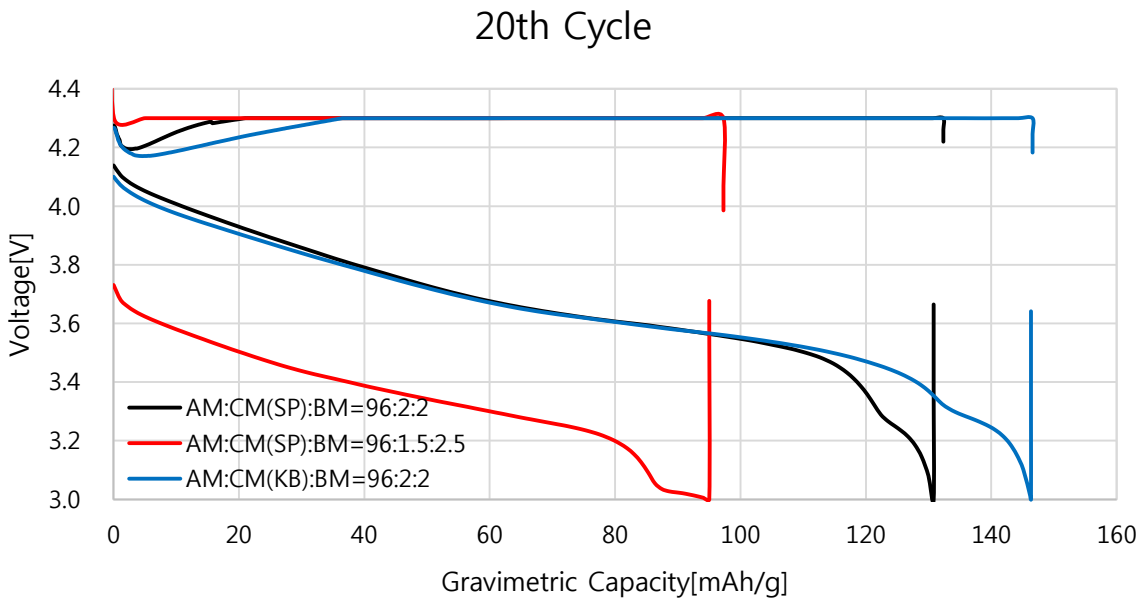

Figure 47. Voltage profile of 20th cycle at 3C rate charging.

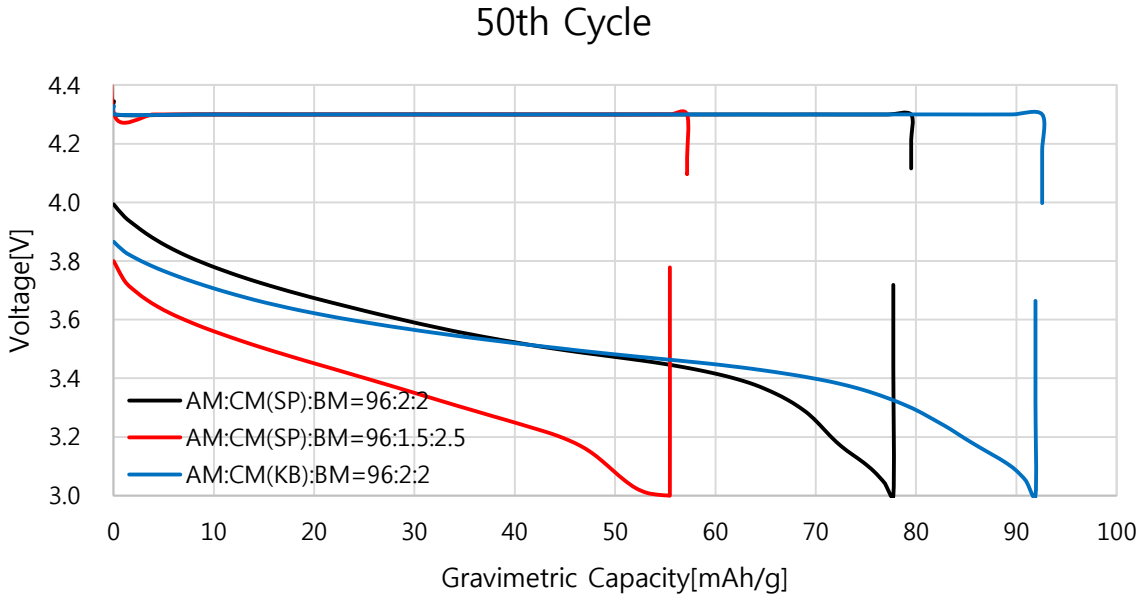

Figure 48. Voltage profile of 50th cycle at 3C rate charging.

2.5% PVDF ratio and 1.5% super P ratio electrode showed the electrical conductivity of 0.0034 S/cm which is 4 times lower than 2% PVDF and 2% super P ratio electrode which showed 0.0126 S/cm. Electrode with the Ketjen Black conducting agent showed the electrical conductivity of 0.0581 S/cm which is 4 times higher than the electrode with super P conducting agent.

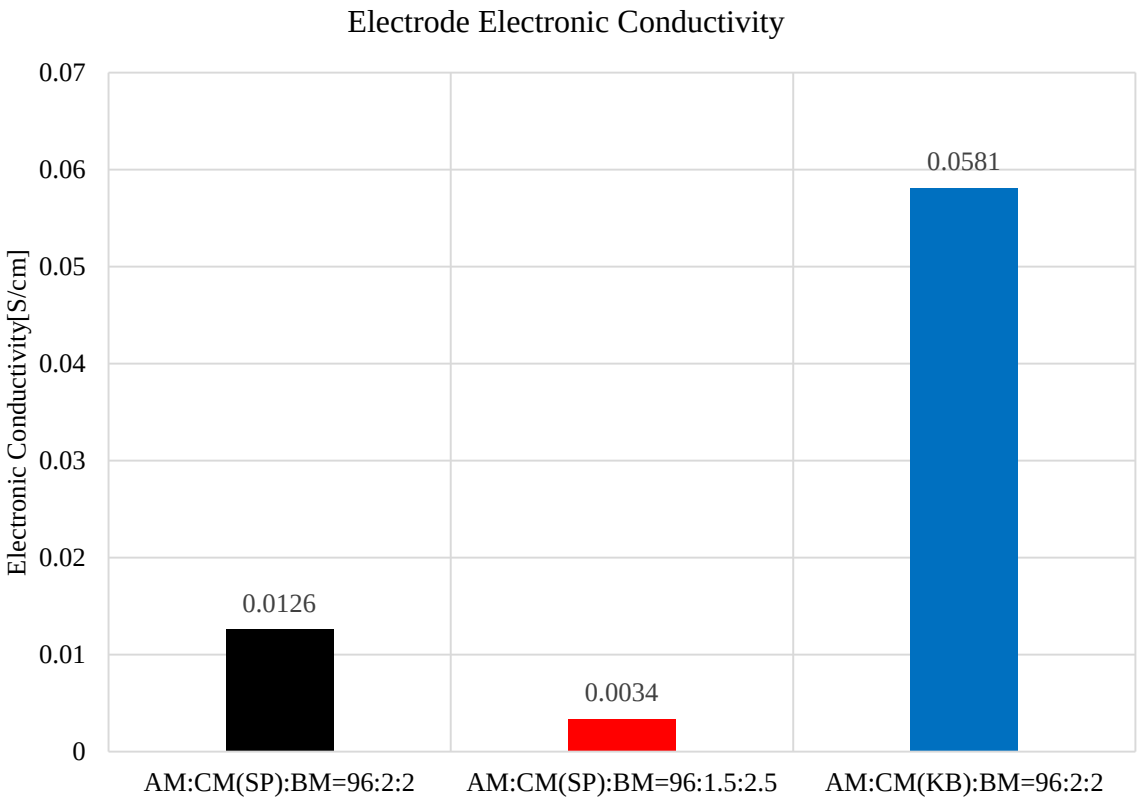

Figure 49. Electrode electronic conductivity of cathode composite.

Table 5. Electronic Conductivity of cathode composite

	AM:CM(SP):BM 96:2:2	AM:CM(SP):BM 96:1.5:2.5	AM:CM(KB):BM 96:2:2
Electronic Conductivity(S/cm)	0.0126	0.0034	0.0581

In figure 50, EIS measurement results show that when the PVDF binder ratio is comparably high, cell impedance is also high. Electrode with the Ketjen Black conducting agent has lower cell impedance because the Ketjen Black conducting agent establishes the well developed conducting network in the electrode. This impedance result is consistent with the electrode electronic conductivity measurement result.

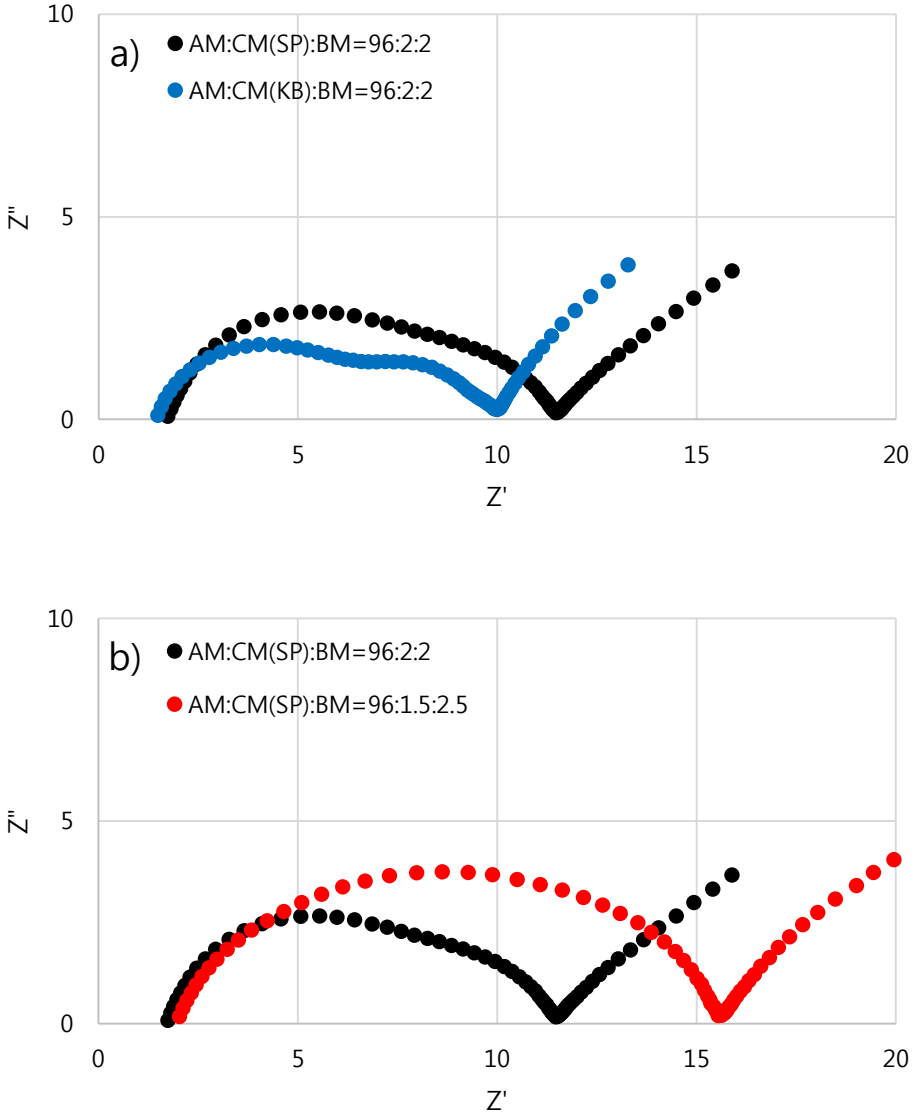

Figure 50. EIS measurement of fresh coin half-cell a) comparing conductive agents and b) composite ratio.

Similar to the anode case, cathode also have the same issues in which the high ratio of face binding structured binder acts as impedance in the electrode composite. Also, since the cathode's active materials have poor electronic conductivity, it needs not only binder but also a conducting agent in the composite. The ratio of the conducting agent is exceedingly important because the establishment of conducting network is highly related to the cycle life and rate capability of cell performance. Therefore, as in anode case, finding the optimizing point of binder and the conducting agent and using the proper ratio of the conducting agent with the high specific surface area would enhance the cell performance.

Ⅳ. Conclusion

In this work, the effect of the binder and the conducting agent in slurry was observed. The amount of active material in the anode and cathode were maintained at 97.4% and 96% respectively to enable application in commercial production. In summary, binder which has face-binding structure in slurry can acts as resistance in the electrode composite. Electrode electronic conductivity measurement and EIS measurement of fresh cell shows that electronic conduction is hindered due to the binder which covers the active material surface. Since resistance increases overpotential in the electrode, initial capacity decreases. However, anode cycle retention and rate capability test shows that the face binding structured electrode has higher retention in both cycle and rate capability. This is because face binding structure has higher mechanical binding strength compared to point binding structured binder. Adhesion test results also show that face binding structured binder has higher mechanical strength in both the cathode and anode. To improve rate capability of lithium ion batteries, a high fatigue strength electrode is needed. To achieve a high fatigue strength electrode, binder which has face binding structure is needed. In case of the cathode, developing a conducting network is essential. Nevertheless, since face binding structured binder has high resistance which is related to high overpotential, it is necessary to adjust binder type, binding structure and ratio.

Ⅴ. Reference

1. Park, J. K., *Principles and Applications of Lithium Secondary Batteries*. 2012.
2. Zheng, H.; Tan, L.; Liu, G.; Song, X.; Battaglia, V. S., Calendering effects on the physical and electrochemical properties of Li[Ni1/3Mn1/3Co1/3]O2 cathode. *Journal of Power Sources* **2012,** *208*, 52-57.
3. Li, C.-C.; Lin, Y.-S., Interactions between organic additives and active powders in water-based lithium iron phosphate electrode slurries. *Journal of Power Sources* **2012,** *220*, 413-421.
4. Goodenough, J. B.; Park, K. S., The Li-ion rechargeable battery: A perspective. *Journal of the American Chemical Society* **2013,** *135* (4), 1167-1176.
5. Dunn, B.; Kamath, H.; Tarascon, J. M., Electrical energy storage for the grid: A battery of choices. *Science* **2011,** *334* (6058), 928-935.
6. Short, G. D.; Bishop, E., Concentration Overpotentials on Antimony Electrodes in Differential Electrolytic Potentiometry. *Analytical Chemistry* **1965,** *37* (8), 962-967.
7. Nitta, N.; Wu, F.; Lee, J. T.; Yushin, G., Li-ion battery materials: Present and future. *Materials Today* **2015,** *18* (5), 252-264.
8. Wu, H.; Cui, Y., Designing nanostructured Si anodes for high energy lithium ion batteries. *Nano Today* **2012,** *7* (5), 414-429.
9. Choi, N. S.; Lee, Y. G.; Park, J. K., Effect of cathode binder on electrochemical properties of lithium rechargeable polymer batteries. *Journal of Power Sources* **2002,** *112* (1), 61-66.
10. Westphal, B. G.; Bockholt, H.; Günther, T.; Haselrieder, W.; Kwade, A. In *Influence of convective drying parameters on electrode performance and physical electrode properties*, ECS Transactions, 2015; pp 57-68.
11. Zheng, H.; Yang, R.; Liu, G.; Song, X.; Battaglia, V. S., Cooperation between active material, polymeric binder and conductive carbon additive in lithium ion battery cathode. *Journal of Physical Chemistry C* **2012,** *116* (7), 4875-4882.
12. Goriparti, S.; Miele, E.; De Angelis, F.; Di Fabrizio, E.; Proietti Zaccaria, R.; Capiglia, C., Review on recent progress of nanostructured anode materials for Li-ion batteries. *Journal of Power Sources* **2014,** *257*, 421-443.
13. Dominko, R.; Gaberscek, M.; Drofenik, J.; Bele, M.; Pejovnik, S.; Jamnik, J., The role of carbon black distribution in cathodes for Li ion batteries. *Journal of Power Sources* **2003,** *119-121*, 770-773.
14. Kwon, N. H.; Yin, H.; Brodard, P.; Sugnaux, C.; Fromm, K. M., Impact of composite structure and morphology on electronic and ionic conductivity of carbon contained LiCoO2 cathode. *Electrochimica Acta* **2014,** *134*, 215-221.
15. Gallagher, K. G.; Trask, S. E.; Bauer, C.; Woehrle, T.; Lux, S. F.; Tschech, M.; Lamp, P.; Polzin,

B. J.; Ha, S.; Long, B.; Wu, Q.; Lu, W.; Dees, D. W.; Jansen, A. N., Optimizing areal capacities through understanding the limitations of lithium-ion electrodes. *Journal of the Electrochemical Society* **2016,** *163* (2), A138-A149.

16. Thomas, M. G. S. R.; Bruce, P. G.; Goodenough, J. B., Lithium mobility in the layered oxide Li1-xCoO2. *Solid State Ionics* **1985,** *17* (1), 13-19.

17. Yazami, R.; Zaghib, K.; Deschamps, M., Carbon fibres and natural graphite as negative electrodes for lithium ion-type batteries. *Journal of Power Sources* **1994,** *52* (1), 55-59.

18. Yoshino, A., The birth of the lithium-ion battery. *Angewandte Chemie - International Edition* **2012,** *51* (24), 5798-5800.

19. Ozawa, K., Lithium-ion rechargeable batteries with LiCoO2 and carbon electrodes: the LiCoO2/C system. *Solid State Ionics* **1994,** *69* (3-4), 212-221.

20. Whittingham, M. S., Lithium batteries and cathode materials. *Chemical Reviews* **2004,** *104* (10), 4271-4301.

21. Kang, K.; Meng, Y. S.; Bréger, J.; Grey, C. P.; Ceder, G., Electrodes with high power and high capacity for rechargeable lithium batteries. *Science* **2006,** *311* (5763), 977-980.

22. Fergus, J. W., Recent developments in cathode materials for lithium ion batteries. *Journal of Power Sources* **2010,** *195* (4), 939-954.

23. Yabuuchi, N.; Ohzuku, T., Novel lithium insertion material of LiCo1/3Ni1/3Mn1/3O2 for advanced lithium-ion batteries. *Journal of Power Sources* **2003,** *119-121*, 171-174.

24. Ohzuku, T.; Brodd, R. J., An overview of positive-electrode materials for advanced lithium-ion batteries. *Journal of Power Sources* **2007,** *174* (2), 449-456.

25. Szczech, J. R.; Jin, S., Nanostructured silicon for high capacity lithium battery anodes. *Energy and Environmental Science* **2011,** *4* (1), 56-72.

26. Pleskov, Y. V., Bard, A. and Folkner, L., Electrochemical methods: Principles and applications, New York: Wiley, 2001. *Elektrokhimiya* **2002,** *38* (12), 1505-1506.

27. Bockholt, H.; Indrikova, M.; Netz, A.; Golks, F.; Kwade, A., The interaction of consecutive process steps in the manufacturing of lithium-ion battery electrodes with regard to structural and electrochemical properties. *Journal of Power Sources* **2016,** *325*, 140-151.

28. Liu, G.; Zheng, H.; Battaglia, V. S.; Simens, A. S.; Minor, A. M.; Song, X., Optimization of Acetylene Black Conductive Additive andPolyvinylidene Difluoride Composition for High Power RechargeableLithium-Ion Cells. *Journal of the Electrochemical Society* **2007,** *6*.

29. Hochgatterer, N. S.; Schweiger, M. R.; Koller, S.; Raimann, P. R.; Wöhrle, T.; Wurm, C.; Winter, M., Silicon/graphite composite electrodes for high-capacity anodes: Influence of binder chemistry on cycling stability. *Electrochemical and Solid-State Letters* **2008,** *11* (5), A76-A80.

30. Choi, N. S.; Yew, K. H.; Choi, W. U.; Kim, S. S., Enhanced electrochemical properties of a Si-based anode using an electrochemically active polyamide imide binder. *Journal of Power Sources* **2008,** *177* (2), 590-594.

31. Koo, B.; Kim, H.; Cho, Y.; Lee, K. T.; Choi, N. S.; Cho, J., A highly cross-linked polymeric binder for high-performance silicon negative electrodes in lithium ion batteries. *Angewandte Chemie - International Edition* **2012,** *51* (35), 8762-8767.

Ⅵ. Acknowledgement

This work was supported by the project from Samsung Research Funding & Incubation Center of Samsung Electronics Co. Ltd (A Rapid Charging Battery and its Prototype Cells Retaining High Energy Density, SRFC-TA1603-01).

Special thanks to dissertation committee assistant referees, Prof. Jaephil Cho and Prof. Nam-soon Choi.

Lastly, I would like to express my sincere appreciation to Prof. Kyeong-Min Jeong.